NSWC/WOL TR 77-175

DDT BEHAVIOR OF GROUND TETRYL AND PICRIC ACID

BY DONNA PRICE
RICHARD R. BERNECKER

RESEARCH AND TECHNOLOGY DEPARTMENT

25 JANUARY 1978

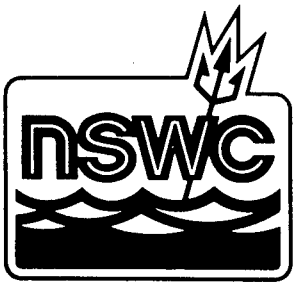

NAVAL SURFACE WEAPONS CENTER

Dahlgren, Virginia 22448 • Silver Spring, Maryland 20910

UNCLASSIFIED

SECURITY CLASSIFICATION OF THIS PAGE *(When Data Entered)*

REPORT DOCUMENTATION PAGE		READ INSTRUCTIONS BEFORE COMPLETING FORM
1. REPORT NUMBER NSWC/WOL TR 77-175	2. GOVT ACCESSION NO.	3. RECIPIENT'S CATALOG NUMBER
4. TITLE *(and Subtitle)* DDT BEHAVIOR OF GROUND TETRYL AND PICRIC ACID		5. TYPE OF REPORT & PERIOD COVERED 6. PERFORMING ORG. REPORT NUMBER
7. AUTHOR(s) Donna Price Richard R. Bernecker		8. CONTRACT OR GRANT NUMBER(s)
9. PERFORMING ORGANIZATION NAME AND ADDRESS Naval Surface Weapons Center White Oak Silver Spring, Maryland 20910		10. PROGRAM ELEMENT, PROJECT, TASK AREA & WORK UNIT NUMBERS 61152N; ZR00001; ZR0130901; WR0119;
11. CONTROLLING OFFICE NAME AND ADDRESS		12. REPORT DATE 25 January 1978 13. NUMBER OF PAGES 62
14. MONITORING AGENCY NAME & ADDRESS*(if different from Controlling Office)*		15. SECURITY CLASS. *(of this report)* UNCLASSIFIED 15a. DECLASSIFICATION/DOWNGRADING SCHEDULE

16. DISTRIBUTION STATEMENT *(of this Report)*

Approved for public release, distribution unlimited.

17. DISTRIBUTION STATEMENT *(of the abstract entered in Block 20, if different from Report)*

18. SUPPLEMENTARY NOTES

19. KEY WORDS *(Continue on reverse side if necessary and identify by block number)*

DDT
Detonation
Sensitivity
Explosives
Picric Acid
Tetryl
Combustion
Flame Spreading

20. ABSTRACT *(Continue on reverse side if necessary and identify by block number)*

This report presents a study of the deflagration to detonation transition (DDT) behavior of ground tetryl to supplement earlier studies on coarse (470μ) and fine (20μ) tetryl. It was found that grinding the coarse tetryl changed the shape and location of the curve, predetonation column length (ℓ) vs. %TMD, and also eliminated the variant behavior of the transition. In contrast to

DD FORM 1 JAN 73 1473 EDITION OF 1 NOV 65 IS OBSOLETE
S/N 0102-LF-014-6601

UNCLASSIFIED

SECURITY CLASSIFICATION OF THIS PAGE *(When Data Entered)*

20. (Cont.)

the fine and coarse tetryls, the ground tetryl appears to follow exactly the physical model of DDT originally describing the transition in 91/9 RDX/wax.

Several shots on picric acid (PA) are also reported; they complete an earlier study. The present results confirm the previous study in that the transition of PA follows the original model and show that its ℓ vs. %TMD curve is, like that of ground tetryl, U shaped. (The branch at higher %TMD lies very close to the curve for fine tetryl.) Finally, the uncommonly long relative detonation time for PA can be attributed entirely to the ignition and burning processes which precede the formation of the first detected compressive wave.

SUMMARY

This work was carried out under task ZR0130901, IR-159. The present results and conclusions on the transition from burning to detonation of granular explosives should be of interest in the areas of explosive sensitivity, reliability, and safety.

This report presents a study of the deflagration to detonation transition (DDT) behavior of ground tetryl to supplement earlier studies on coarse (470μ) and fine (20μ) tetryl. It was found that grinding the coarse tetryl changed the shape and location of the curve, predetonation column length (ℓ) vs. %TMD, and also eliminated the variant behavior of the transition. In contrast to the fine and coarse tetryls, the ground tetryl appears to follow exactly the physical model of DDT originally describing the transition in 91/9 RDX/wax.

Several shots on picric acid (PA) are also reported; they complete an earlier study. The present results confirm the previous study in that the transition of PA follows the original model and show that its ℓ vs. %TMD curve is, like that of ground tetryl, U shaped. (The branch at higher %TMD lies very close to the curve for fine tetryl.) Finally, the uncommonly long relative detonation time for PA can be attributed entirely to the ignition and burning processes which precede the formation of the first detected compressive wave.

Julius W. Enig

JULIUS W. ENIG
By direction

CONTENTS

ILLUSTRATIONS

ILLUSTRATIONS (Cont.)

TABLES

I. INTRODUCTION

The present work is a continuation of the study of the deflagration to detonation transition (DDT) in pure explosives and the effect of particle size on such transitions. In particular, it supplements Reference 1 which presented the results obtained with fine tetryl (20μ), coarse tetryl (470μ), and picric acid. Although fine and coarse tetryl both showed a variation from the physical model proposed earlier for DDT[2], the variation could be explained in terms of the chemistry of tetryl decomposition at relatively low temperatures[1]. Moreover, addition of 3% wax to the tetryl so changed the process that 97/3 tetryl/wax appeared to conform to the original model. I.e., the waxed tetryl showed a rapid pressure rise in the ignition region[1,3] whereas the coarse and fine tetryls showed rapid pressure buildup nearer the site of detonation onset than the ignition region.

The tetryl used in the present work was prepared from the coarse tetryl of the earlier work by grinding. Its transitional behavior seems to follow that proposed in the original physical model. Thus, initial particle size distribution has a large effect on the observed DDT mechanism as well as on the predetonation column length (ℓ) as a function of %TMD.

The additional data on picric acid (PA) complete the planned series of experiments on that material. They also provide further detail on the unusually long interval between formation of the convective and postconvective (PC) fronts during transition in that material.

---

1. Price, D., Bernecker, R. R., Erkman, J. O., and Clairmont, A. R., "DDT Behavior of Tetryl and Picric Acid," NSWC/WOL TR 76-31, 21 May 1976.
2. Bernecker, R. R., and Price, D., Combustion and Flame Vol. 22, 119-129 and 161-170 (1974). See also NOLTR 72-202.
3. Price, D., and Bernecker, R. R., "DDT Behavior of Waxed Mixtures of RDX, HMX, and Tetryl," NSWC/WOL TR 77-96, 18 Oct 1977.

II. EXPERIMENTAL ARRANGEMENT AND PROCEDURE

The experimental setup and procedures have been described in detail elsewhere[1,2]. A schematic of the arrangement is shown in Figure 1. It consists of a seamless steel tube with heavy end closures. The column length of the 0.35 g of 25/75 B/KNO_3 ignitor is 6.3 mm; the length of the explosive column is 295.4 mm.

The present tetryl (844) was prepared by grinding the coarse tetryl (812) underwater in a ball mill for an hour. Figure 2 consists of several photomicrographs of the ground material. They show many particles of 200-300μ, which survived the grinding, and much finer material down to 10μ and less. A sieve analysis, given in Appendix A, indicated a weight mean particle size of $\bar{\delta} \sim 160\mu$. However, this value must be considered suspect because the Preparation Group was subsequently unable to obtain a sieve cut ($\bar{\delta} \sim 115\mu$) or carry out any other sieving operations on this tetryl. It exhibited enough static charge to clog the screen openings despite the electrical grounding of the sieves. Because of this and because very few particles of 100-160μ are evident in Figure 2, tetryl 844 is called "ground tetryl" and no average size is assigned. The picric acid used is 835 ($\bar{\delta} \sim 67\mu$); it is the same batch used for the previous work, and its sieve analysis appears in Reference 1.

The DDT tube is instrumented with ionization probes and strain gages to monitor ionization fronts and internal pressure, respectively. For brevity, henceforth ionization probes will be referred to as probes; strain gages, as gages. As before[1], both custom-made and commercial probes are used; distance-time (x-t) data from each are distinguished on the graphs. The number of gage locations for monitoring internal pressure is now an average of four or five per tube. The gage output is reported in strain (ε) or microstrain (με). In a static calibration of the tube, the gradient is 112 με/kbar up to the elastic limit at 2.2 kbar. From 2 to 4.7 kbar, the microstrain increases from 225 to 788.

All procedures and data reduction are those of Reference 1 and are completely described there or in Reference 2.

III. EXPERIMENTAL RESULTS AND DISCUSSION

A. Ground Tetryl

Nine shots were made on the ground tetryl. Detailed data and records are given in Appendix B; they are summarized in Table 1. As indicated there, five sets of records indicated transitional behavior described by the original DDT model[2]; these included one shot (No. 1015) that did not show DDT in the regular tube but did show a convective wave front and a PC front originating near the ignition area. Only one shot of the nine (No. 615) had records suggesting the variant behavior observed with fine and coarse tetryl.

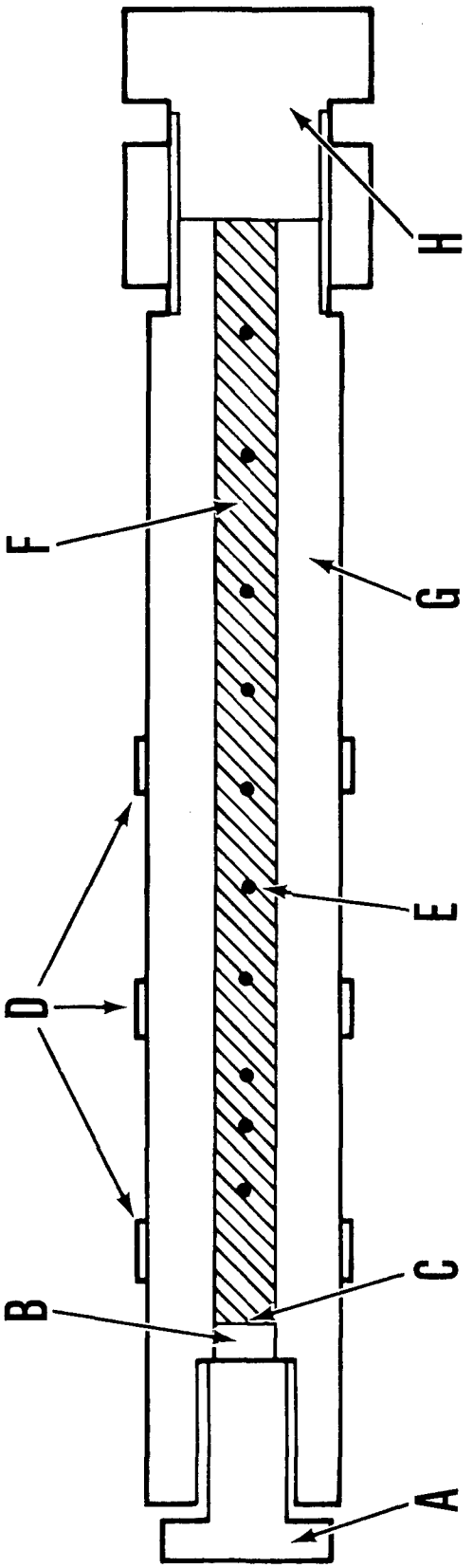

FIGURE 1 CROSS SECTION OF DDT TUBE. (A. IGNITOR BOLT; B. IGNITOR; C. IGNITOR/EXPLOSIVE INTERFACE; D. STRAIN GAGES; E. IONIZATION PROBE LOCATION; F. EXPLOSIVE CHARGE; G. TUBE; H. BOTTOM CLOSURE. INNER DIAMETER = 16.3 mm, OUTER DIAMETER = 50.8 mm, DISTANCE FROM IGNITOR/EXPLOSIVE INTERFACE TO BOTTOM CLOSURE = 295.4 mm.)

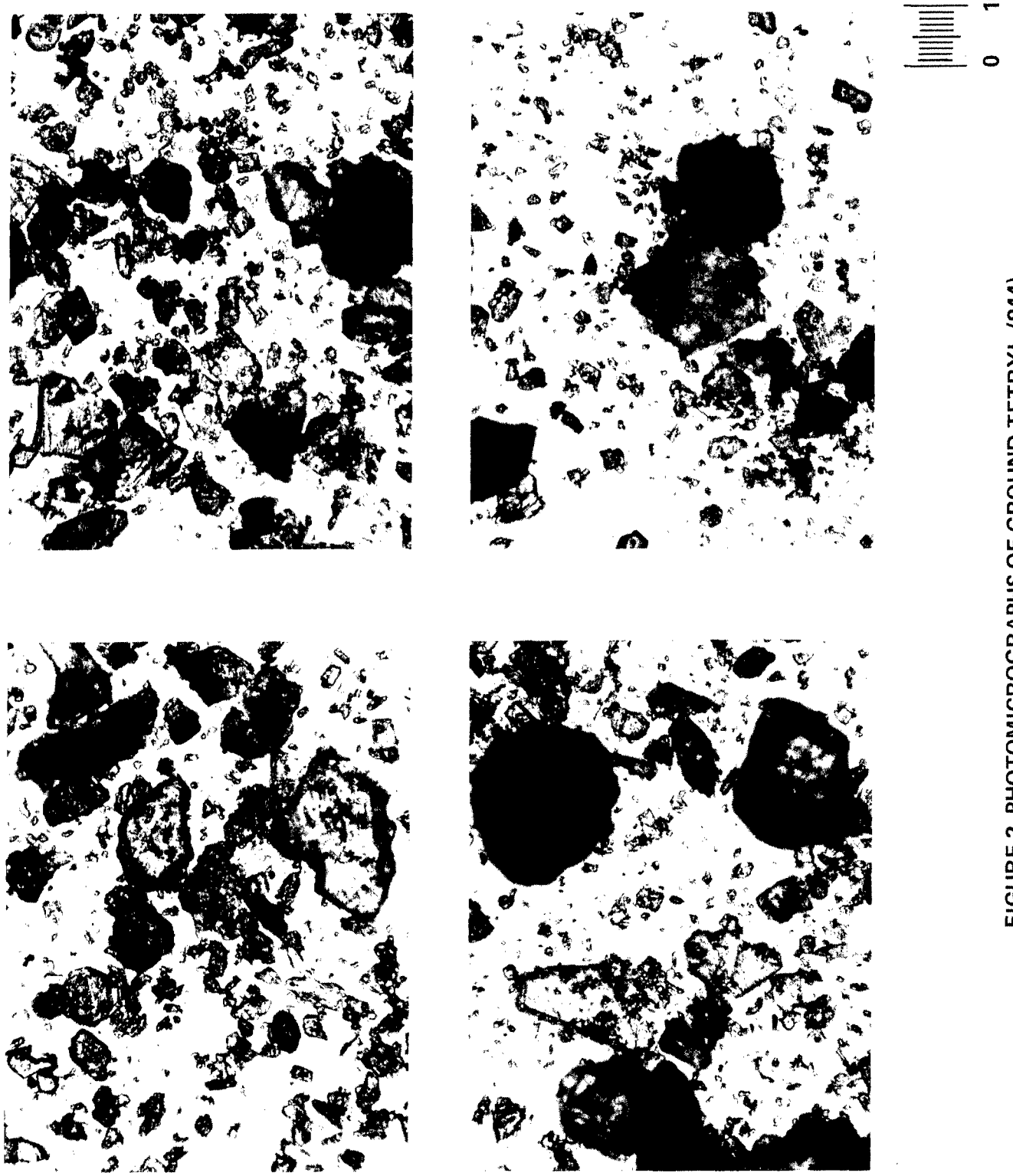

FIGURE 2 PHOTOMICROGRAPHS OF GROUND TETRYL (844)

Table 1

SUMMARY OF DATA ON GROUND TETRYL (844)

Shot No.	ρ_o g/cm^3	%TMD	Velocities, mm/μs b[a]	First Comp. Front	Second Comp. Front	D	ℓ mm	Relative Times, μs Δt_D	Δt_P	Δt_E	Apparent Mechanism
1015	1.55	89.8	0.5	1.2	-	F	F	-	-	-	model
1313	1.51	87.5	0.7	1.1	2.4	7.7	225	172	108	64	model
614	1.46	84.6	1.1	0.98	-	7.5	120	66	-	-	c
1113	1.40	81.0	1.4[b]	2.4	-	7.2	146	95.3	50	45	model
1512	1.32	76.5	0.21	1.4	1.7	7.1	145	174	91 121	83 53	model[d]
1114	1.32	76.5	0.86	-	-	6.5	78	33	-	-	c
615	1.28	74.2	0.23[b]	0.79	1.7	6.5	115	108	-	-	variant?
1112	1.13	65.5	0.32[b]	1.3	-	5.6	168	341	182	159	model
1307	1.06	61.0	0.22	0.42	-	5.5	182	566	327	239	c

a) $\Delta x/\Delta t$ for first two IPs.
b) Data from second two IPs or later.
c) Insufficient data for classification.
d) Two forward moving compressive waves observed.

In contrast to this, records of three out of eight shots on coarse tetryl[1] showed the variant behavior and only one suggested the original model. Similarly, records of four out of ten shots on fine tetryl[1] showed the variant behavior and only one suggested the model. Hence, the mixture of fines with coarse particles (Figure 2) seems to have changed the DDT behavior from the variant to that of the original model.

The dashed curve of Figure 3 shows the variation of the predetonation column length (ℓ) with percent theoretical maximum density (%TMD) for the ground tetryl; also shown are the curves obtained earlier for fine (20μ) and coarse (470μ) tetryl. It is obvious that the present data show very large scatter. We attribute this to the heterogeneity of the material (see Figure 2) as contrasted to the unimodal, narrow particle size distribution found for both the fine and coarse tetryls. Addition of the fines from grinding to the surviving coarse material evidently results in an ℓ vs. %TMD relation which approximates the behavior of fine tetryl at high porosities and of coarse tetryl at lower porosities. Alternatively (or in addition), crushing the coarse particles of tetryl during the pressing operation may result in a final particle size distribution more closely approximating that of the ground tetryl than that of the fine.

Korotov et al.[4] investigated DDT in porous PETN, both fine (20μ) and coarse (500μ). They found that ℓ vs. %TMD exhibited a minimum, as do our curves for 91/9 RDX/wax[2] and 94/6 RDX/wax[3]. Indeed, both coarse and fine tetryl have ℓ vs. %TMD curves showing a minimum {Reference 1 and Figure 3}. However, for PETN, the value of ℓ was practically the same at both minima, and the shift in curves was such that at 70% TMD ℓ(fine) > ℓ(coarse) whereas at 60% TMD ℓ(fine) < ℓ(coarse). The situation for unimodal tetryl is more complicated. The curve for coarse tetryl has a minimum at about 70% TMD and most resembles the PETN curves. But the curve for fine tetryl does not have the same form, and from the available data[1] it is difficult to say whether it shows a true minimum or a plateau. Certainly ℓ(fine) > ℓ(coarse) over the entire range of compaction. This result, in marked contrast to those reported for PETN, might arise from the lesser sensitivity and lower reaction rate of the tetryl as well as from the scatter of the PETN results. The ground tetryl too shows great scatter, but apparently follows the form of the PETN curves better than either the coarse or the fine. This might, in the case of both PETN and ground tetryl, be an effect of the greater range in particle size than found in either the coarse or the fine tetryl. If so, the behavior of the ground tetryl might be reproduced by some mixture of the fine and coarse materials.

4. Korotkov, A. I., Sulimov, A. A., Obmenin, A. V., Dubovitskii, V. F., and Kurkin, A. I., "Transition from Combustion to Detonation in Porous Explosives," Combustion, Explosion, and Shock Waves, Vol. 5, 216-222 (1969).

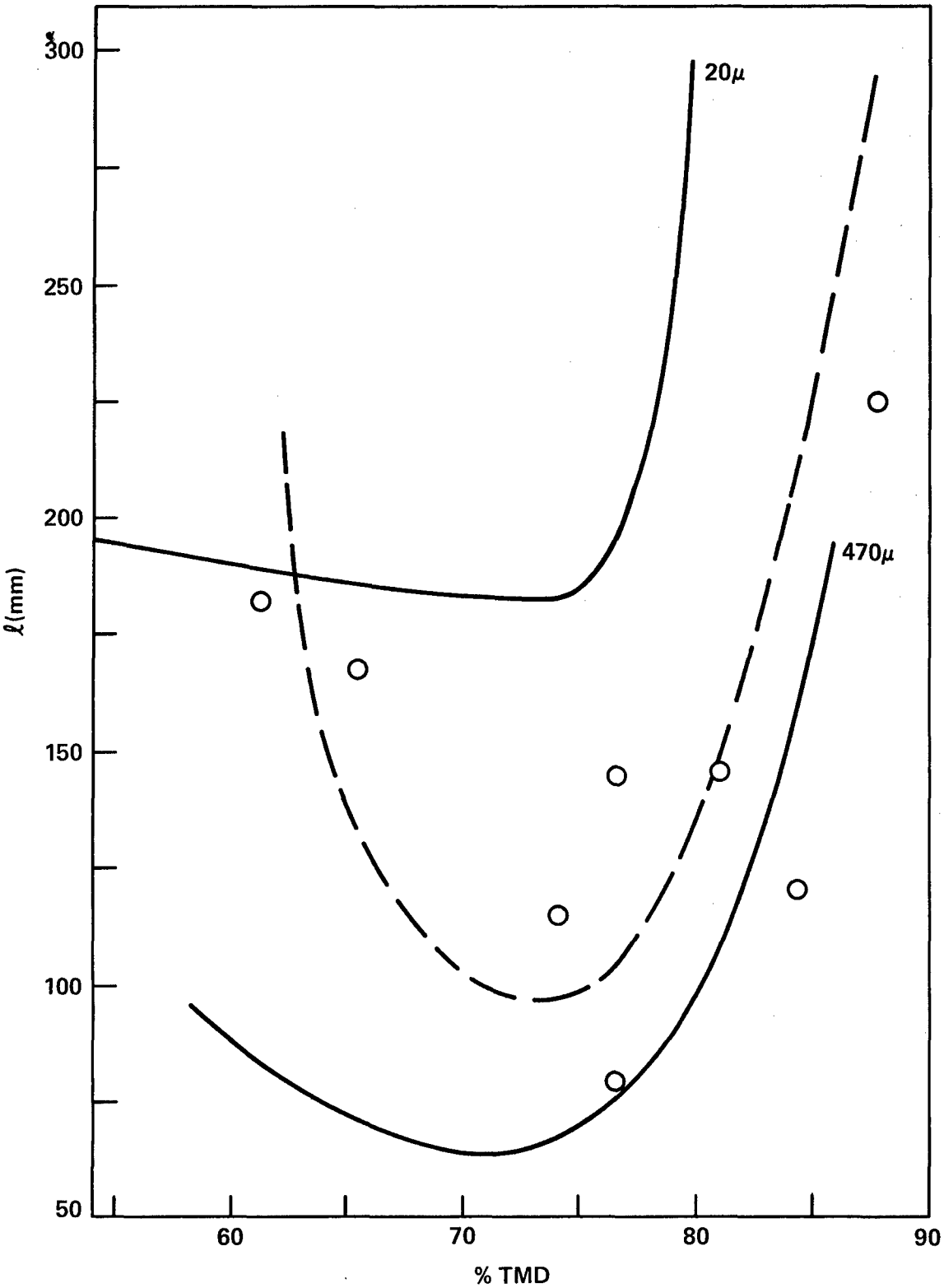

FIGURE 3 VARIATION OF PREDETONATION COLUMN LENGTH WITH POROSITY OF GROUND TETRYL COMPARED TO THAT OF COARSE AND FINE TETRYL

The minimum of the curve for ground tetryl seems to be at a higher ℓ value and about the same %TMD as the corresponding value for the coarse tetryl.

Another variable of importance in DDT is the relative time to detonation Δt_D; it is the time between the response of a specific IP (generally the trigger probe) and the onset of detonation. In many cases, there is a correlation between ℓ and Δt_D as there is for the coarse and fine tetryls over the porosity range examined. (The correlation has to be established in each new situation because it is not always evident e.g., no such correlation could be found for a constant composition waxed RDX or HMX over a range of compaction[3].) Moreover, if Δt_D is plotted vs. %TMD, the fine and coarse tetryls both have U shaped curves with respective minima at 69 and 73.5% TMD (see Figure 4, Table 1, and Tables 1 and 2 of Reference 1; note that Δt_D is referred to the probe at 41 mm for the coarse and ground tetryl, but to that at 60 mm for the fine). In Figure 3, the ℓ as %TMD curves drawn show minima at 74 and 71% TMD for the fine and coarse tetryl, respectively. However, these curves represent estimates of the best fit to the data. Reference to the original data (Figure 1 of Reference 1) shows that the curves could have been drawn to show minima at 69 and 73.5% TMD. In fact, fine tetryl showed the smallest experimental value of ℓ at 45.8% TMD, not at either 69 or 73.5% TMD. Because of their better resolution of the minima, the curves Δt_D vs. %TMD have improved the location of minima in the curves of Figure 3 for fine and coarse tetryl. However, they merely confirm the general location of the curve for ground tetryl between the other two since the large scatter in these data is, of course, still evident.

The location of the minima in the ℓ vs. %TMD curve places that for the fine tetryl at a higher %TMD than that for the coarse. That too was the case in the reported PETN data[4]. But the two U shaped curves for PETN overlapped in some sections whereas the curves for fine and coarse tetryl do not intersect.

It remains to be seen if a mixture can be made of the fine and coarse tetryl to duplicate the behavior of the ground tetryl. Meanwhile, the present results indicate the inadequacy of a weight mean diameter ($\bar{\delta}$) to represent the particle size distribution in a ground material, and, indeed, the use of such a material in studying the effects of particle size. It is distinctly preferable to use materials showing a very narrow range in δ (e.g., the coarse and fine tetryls of Reference 1) in assessing particle size effects. However, it is generally too expensive to prepare large amounts of such materials by sieving a supply of the explosive having a wide range in particle size (as many production samples or ground samples do). Moreover, it is generally too expensive to use a controlled recrystallization process. What is needed is equipment such as a fluidized energy mill which can be set to grind to a specified narrow range of particle size. It is reported that such mills are now used by the larger propellant manufacturers, but none is as yet available in a Navy facility.

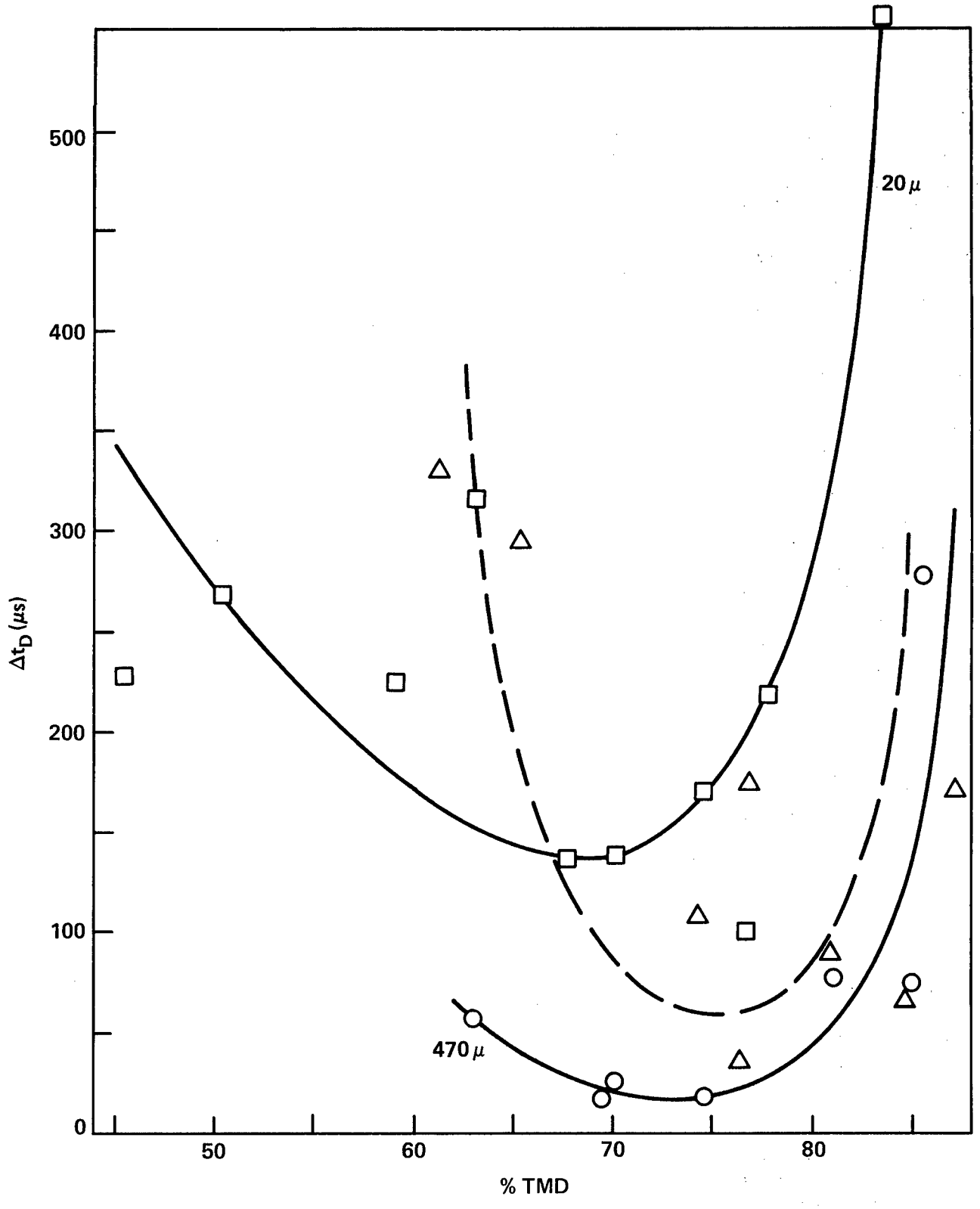

FIGURE 4 VARIATION OF RELATIVE TIME TO DETONATION WITH POROSITY OF GROUND TETRYL COMPARED TO THAT OF FINE AND COARSE TETRYL (○ COARSE TETRYL; □ FINE TETRYL; △ GROUND TETRYL)

B. Picric Acid

The first portion of our study of the DDT behavior of picric acid was reported in Reference 1. We found that in a number of cases the convective flame front appeared to fail before it reached the end of the charge; nevertheless, a transition occurred at a comparatively large relative time to detonation Δt_D. Strain gage records frequently exhibited a number of plateaus indicating compaction of the charge, and a rearward compression from the region of shock formation or detonation was often detected. Finally, the predetonation column length ℓ was comparable to that of the fine tetryl, although Δt_D was much greater. The transition mechanism appeared to be that of the original model[2].

Summary data for the additional shots are presented in Table 2. They have confirmed all the initial observations as well as contributed greater detail which will be described for each shot of the present data. For convenience, the data of Reference 1 have also been included in the table.

Shot 1402 (Figure C1) extended the compaction range for successful transition up to 77.4% TMD. This shot had a normal rate for the convective and PC fronts, showed incipient plateaus in the SG records, and had a rearward travelling reflection at 6.7 mm/μs. Although that value is within 10% of the detonation velocity, the ignitor end of the DDT tube was relatively intact. Hence, the rearward wave seems to be a shock, not a retonation. Finally, the mechanism appears to be that of the initial model.

At the other end of the porosity scale, three shots have been fired: 811, 1504, and 1514 at 62-63% TMD. The first two were in regular length DDT tubes. Shot No. 811 was reported a failure[1] and is so labeled in Table 2. However, this was a case in which IP data and tube fragmentation, dent in the closure bolt, and tube wall markings were in conflict. Consequently, the shot is labeled F, but the location of change in wall pattern and time of recording have also been noted.

Shot 1504 (Figure C3) was a replicate of 811 and showed much the same results: a falling off of the velocity of the convective front and SGs triggered in the usual manner, indicating $p \leq 0.3$ kbar during the recording interval. However, at some later (and unknown) time a probe in a special circuit* triggered backup scopes to

*The special circuit probe was not recorded on the IP record; hence, it is assumed to have responded after that record ended. Although the circuit was designed to obtain response of the probe at higher resistance fronts than the usual convective front, the circuit was at this time in an early development stage. Thus, the probe response was sometimes very late as in this case and in Shot 1418 where it was not recorded at all, and sometimes responded as in Shot 1514 (Figure C2) where it appeared to differ very little from the custom-made probes.

Table 2

SUMMARY OF DATA ON PICRIC ACID (ρ_v = 1.76 g/cc)

Shot No.	ρ_o g/cm^3	%TMD	B[a] mm/μs	2C x 10^3 mm/μs^2	V_{PC} mm/μs	ℓ mm	D mm/μs	$^{41}\Delta t_D$ μs	$^{41}\Delta t_p$ μs	$^{41}\Delta t_E$ μs
				($\bar{\delta}$ ∿ 67μ), Lot 835						
1014*	1.58	90.0	∿1.0	-	-	-	F	-		
1402	1.36	77.4	0.28	0.38	1.1	196	6.20	333	194	139
1205*	1.32	75.1	0.32	-0.18	1.9	215	6.14	652	532	120
1108*	1.25	70.9	0.21	-0.11	1.1	180	5.71	1178	1017	161
916*	1.21	68.9	∿0.15	-	1.0	163	5.70	885	745	140
1204*	1.17	66.5	0.20	-0.15	1.0	174	5.71	1040	896	144
1514[b]	1.10	62.7	∿0.15	-	-	279[b]	5.21	1890	-	-
811*	1.10	62.4	∿0.20	<0	-	(215±2)[c]	F	(>1122)[c]	-	-
1504	1.09	61.9	0.19	-0.04	-	(242±6)[c]	F	(>1470)[c]	-	-
				Narrow Sieve Cut, $\bar{\delta}$ = 115μ						
1407	1.20	68.4	∿0.44		1.5	229	5.6	361	221	140
1418	1.21	68.8	0.29	-0.17	1.0	192	6.40	960	787	173

*Reported in Reference 1.

a) From fit to $x = A + Bt + Ct^2$

b) Extra length tube (18 in.) without strain gages

c) These shots were labelled failures although tubes were marked at indicated ℓ value. See discussion in text.

Δts are times relative to discharge time of probe at x = 41 mm. Subscripts D, p, and E refer, respectively to detonation, pressure front, and the difference ($\Delta t_D - \Delta t_p$).

record data for the first three SGs. These records, shown in Figure C3b, indicate a compression wave travelling toward the ignitor at a velocity of 1-2 mm/μs. Moreover, the tube walls indicate detonation at ℓ = 242 mm although the marking is not as clear as that of Shot 811 nor is the fragmentation as great. From the damage, it does not seem that a retonation occurred. On the other hand, there is no conclusive evidence that a detonation did not occur after a long delay time and during a period greater than the recording time.

Shot 1514 was another replicate of the charge (62.7% TMD), but was fired in a longer (18 in.) DDT tube instrumented with IPs but no SGs. This charge definitely showed a transition to detonation in its IP record (Figure C2).

Figure 5 summarizes the ℓ vs. %TMD data for Lot 835 PA ($\delta \sim 67\mu$). The solid curves are for fine and coarse tetryl, as marked. The dashed curve is an estimate of the PA curve. Although the two shots at 62% TMD, which showed ambiguous results, have been plotted as squares (other data points are circles), they have little influence on the location of the low %TMD branch of the curve. Picric acid appears to have a typical U shaped ℓ vs. %TMD curve with a minimum near 70% TMD. Its shape is similar to that of the ground tetryl and of those drawn for PETN[4]*. The ℓ values for PA are approximately the same as those of the fine tetryl down to 65% TMD.

The parameter that illustrates most significantly the difference in the DDT behavior of PA compared to tetryl or any of the other HE so far investigated is relative time to detonation Δt_D**. To demonstrate this, available data (at 70% TMD only) have been assembled in Table 3 and plotted as Δt_D vs. ℓ in Figure 6. All Δt_D values are relative to discharge time of the IP at 41 mm. Consequently, pure HE such as RDX, HMX, PETN, TNETB, etc. with $\ell \sim 41$ mm and hence ${}^{41}\Delta t_D \sim 0$ have been omitted. Only an upper limit curve (for the waxed series of Reference 3) has been drawn. All other HE fall on or below this curve whereas PA lies above it, i.e., $\Delta t_D(\text{PA}) \sim 3 \times \Delta t_D(\text{another HE with } \ell = 172 \text{ mm})$.

The interval Δt_D is made up of (1) Δt_p, the time between the formation of the (first) convective flame front and the formation of the (first compressive) PC front and (2) Δt_E, the time between the formation of PC compression front and the onset of detonation.

*PETN is a very sensitive explosive and exhibits very small ℓ values; consequently, the measured ℓ values show greater scatter and less precision than those for PA. The scatter for PETN more closely resembles that for ground tetryl.

**In marked contrast to the data for the tetryls, the PA results do not produce a curve Δt_D vs. %TMD similar to the ℓ vs. %TMD curve. The PA data Δt_D vs. %TMD show, at most, a point of inflection; no minimum is evident.

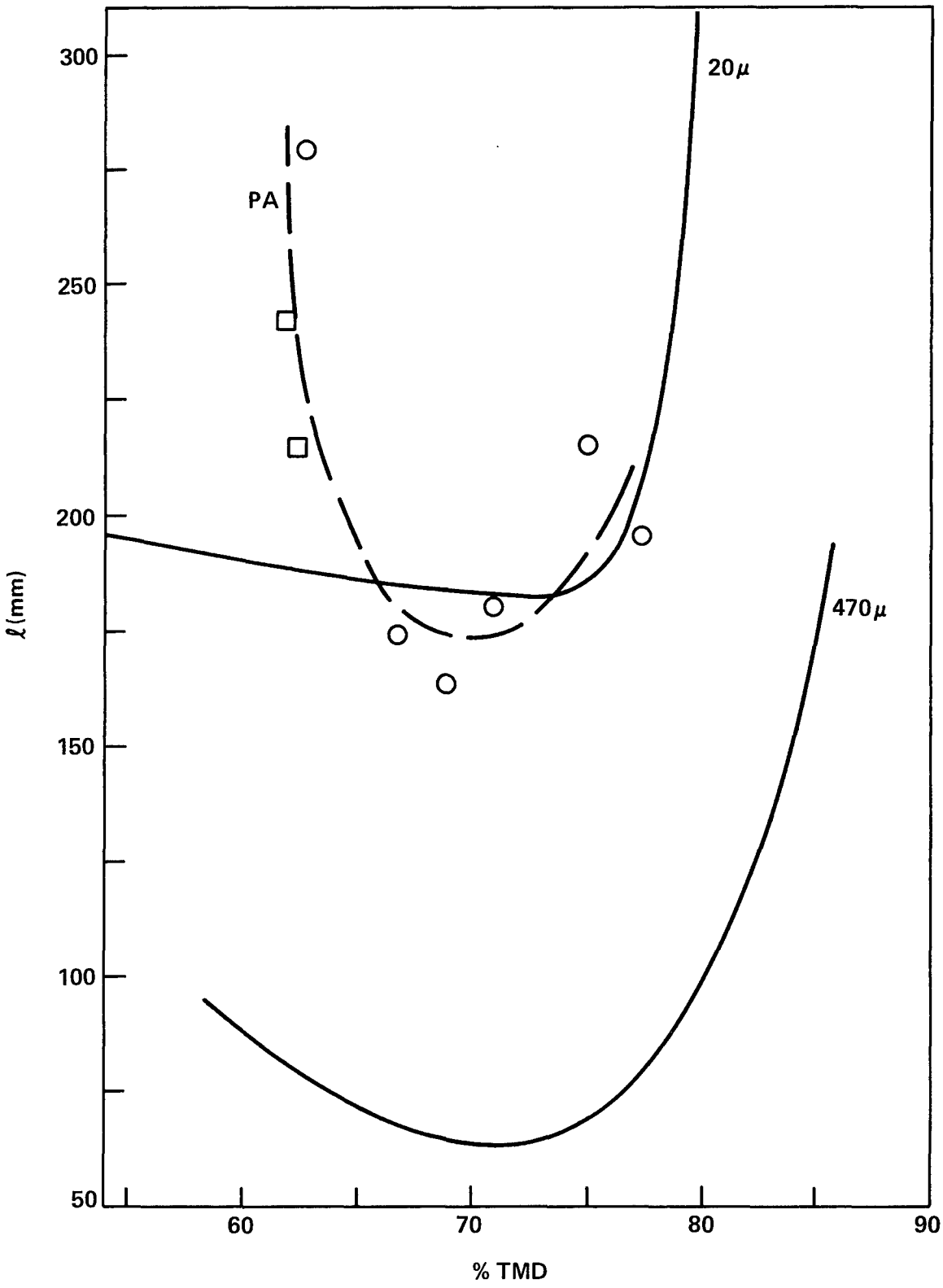

FIGURE 5 VARIATION OF PREDETONATION COLUMN LENGTH WITH POROSITY OF PICRIC ACID COMPARED TO THAT OF FINE AND COARSE TETRYL

Table 3

AVAILABLE ℓ, Δt DATA FOR CHARGES AT 70% TMD

H.E.	ℓ mm	$41\Delta t_D$	$41\Delta t_E$	Reference
91/9 RDX/wax	275	~610	127	NOLTR 72-202
94/6 RDX/wax	135	182	-	NOLTR 72-202
97/3 RDX/wax	95	79	-	NOLTR 72-202
Tetryl (450 μ)	64	21	-	Read from curves of Figures 3 & 4
Tetryl (20 μ)	184	139	-	Read from curves of Figures 3 & 4
Tetryl (ground)	103	86	-	Read from curves of Figures 3 & 4
PA (67μ)	172	1031	150	Average value, Table 2
97/3 RDX (A)/wax	72	32.5	31	NSWC/WOL/TR 77-96
94/6 RDX (A)/wax	130	186	89	NSWC/WOL/TR 77-96
91/9 RDX (A)/wax	220	550	140	NSWC/WOL/TR 77-96
HMX/Wax (115 μ)				
3	67	22	22	NSWC/WOL/TR 77-96
6	99	87	56	NSWC/WOL/TR 77-96
9	143	197	117	NSWC/WOL/TR 77-96
12	273	~569	314	NSWC/WOL/TR 77-96
HMX(A)/Wax				
6	119	144	81	NSWC/WOL/TR 77-96
9	210	395	179	NSWC/WOL/TR 77-96
NC	165	145	35	Not yet reported

If Δt_E is considered instead of Δt_D, PA behaves much like other HE (see Figure 7). Its Δt_E and ℓ approximate those of 91/9 HMX/wax among the HE for which we have the data. (Its ℓ also approximates that of 70% TMD fine (20μ) tetryl for which Δt_E cannot be measured.) Hence, as in the previous report, the evidence is strong that PA differs from other HE chiefly in its resistance to ignition and propagating combustion. Once a sufficient amount has burned in such a manner as to form the PC (compression) wave, the rest of the transition occurs as rapidly as in any comparable explosive (e.g. 91/9 HMX/wax).

The last two shots listed in Table 2 were made at about 70% TMD on a narrow sieve cut ($\bar{\delta} \sim 115\mu$) taken from PA 835 ($\bar{\delta} \sim 67\mu$). The data are plotted in Figures C4 and C5. Both sets of records show features observed in the 66-71% TMD range in the previous work[1]. For example, Shot 1407 shows a shock from the detonation area travelling toward the rear, and Shot 1418 shows the familiar failure of the convective front to propagate in PA. In both C4a and C5a, the PC front has been drawn as a compression originating at some $x < 70$ mm. In both cases it could have been drawn as part of an explosive event originating at about 78 and 50 mm, repectively. This has not been done because none of the other PA records suggest anything but the usual DDT model and because the indication of a different behavior here is not great.

If we average the values of ℓ for these two shots, we obtain $\bar{\ell} = 210$ mm at 68.6% TMD whereas the curve of Figure 5 shows $\ell = 175$ at this porosity. Hence, the 115μ material shows a 20% higher value of ℓ than the 67μ PA. This is hardly significant if normal scatter is ±10% ℓ. Most of our experiments at 70% TMD have shown a decrease of ℓ with an increase in $\bar{\delta}$. Earlier we described the U shaped ℓ vs. %TMD curves for PETN, their shift with change in δ, and their intersection. We have also demonstrated here U shaped curves for ground and coarse tetryl as well as PA. It follows that we really cannot predict a particle size effect on ℓ for any specific explosive at any given %TMD. In the present work, we are not sure that removing the fines from PA ($\bar{\delta} \sim 67\mu$) has had any effect on its ℓ value.

To examine the particle size effect on Δt, the values Δt_E vs. %TMD from Table 2 are plotted in Figure 8. The two values for the 115μ PA are shown as solid points, the rest are open. The trend is decreasing Δt_E with increasing %TMD, but the scatter is large - again a spread of about 20% or ±10% for each experiment. Shots 1407 and 1418 are respectively at the lower and upper boundaries of the scatter range. Hence, the particle size effect on Δt_E also seems to be experimentally insignificant.

Finally, examination of C5a and b shows that in the long interval of propagation and failure of the convective front, SG records show very low pressures. Thus the apparent failure could be caused by a pulsating burning such as that observed by Fogel'zang el al[5] at

5. Fogel'zang, A. E., Margolin, A. D., Kolyasov, S. M., and Khasyanov, Kh. Zh., "Combustion of Picric Acid" ibid., Vol. 11 No. 6, 719-26 (1974).

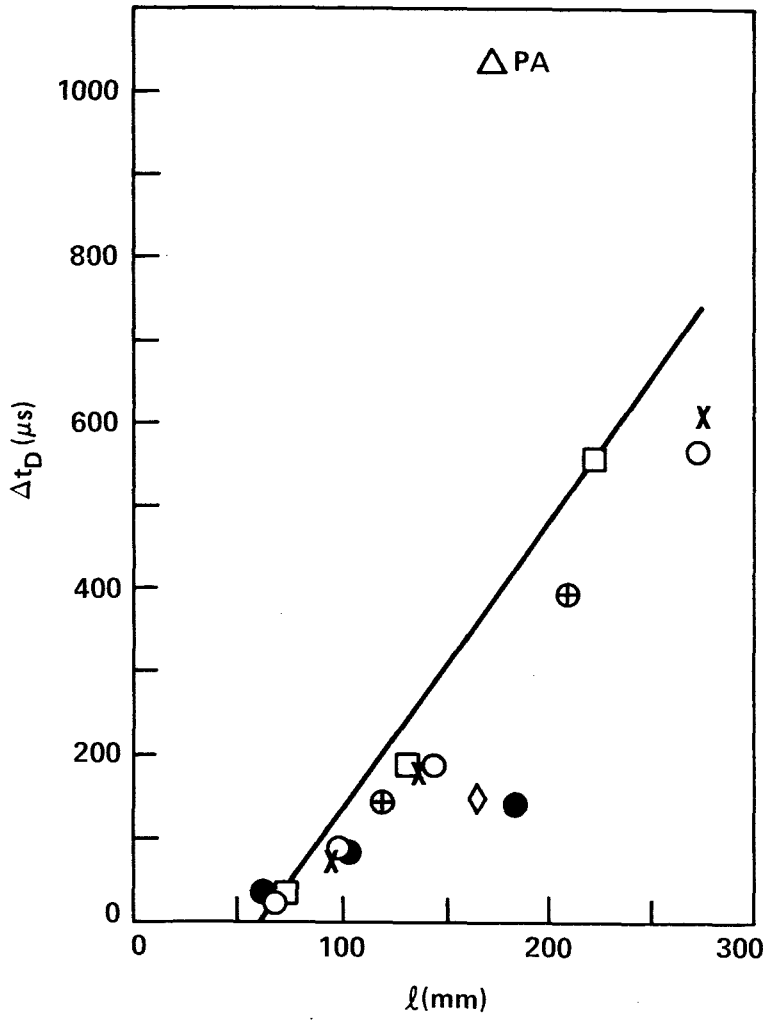

FIGURE 6 VARIATION OF Δt_D WITH ℓ FOR 70% TMD CHARGES (X WAXED RDX SERIES, NOLTR 72-202; □ WAXED RDX SERIES, ○ WAXED 115μ - HMX, ⊕ WAXED HMX (A)- NSWC/WOL/TR 77-96; ◊ NITROCELLULOSE; ● TETRYL; △ PICRIC ACID)

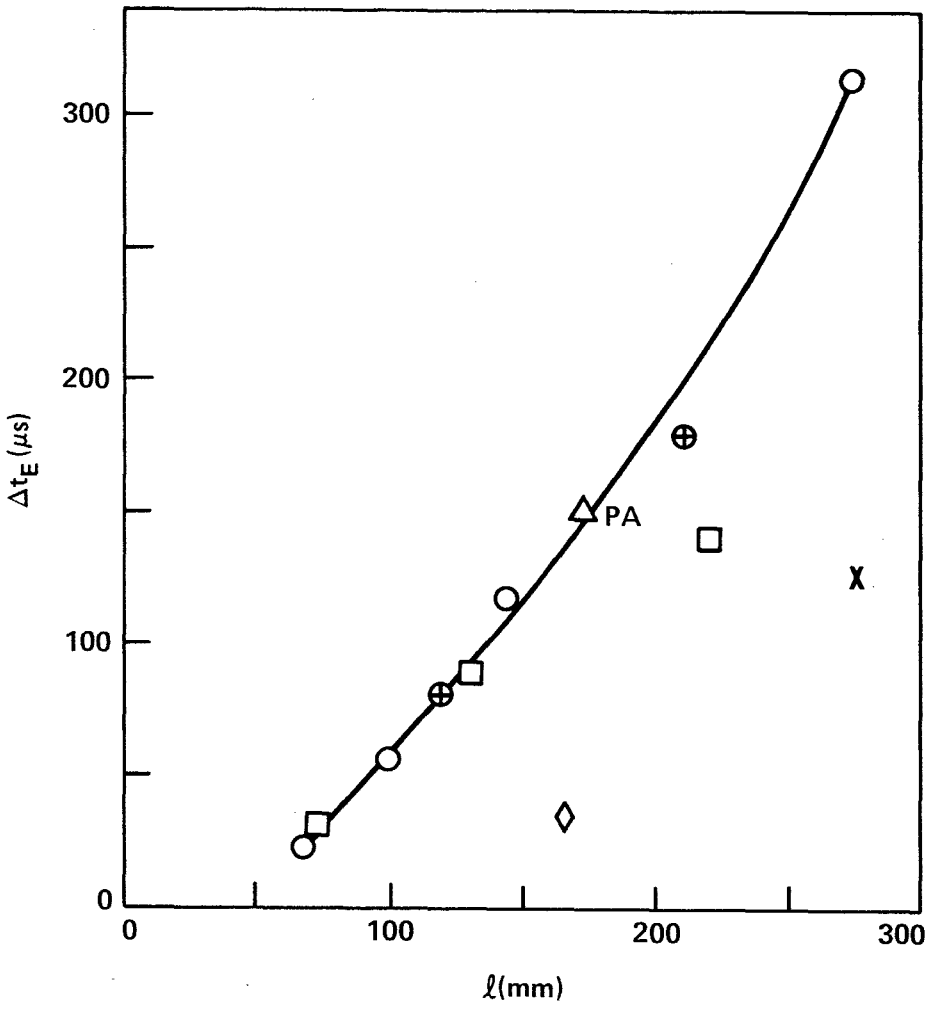

FIGURE 7 VARIATION OF Δt_E WITH ℓ FOR 70% TMD CHARGES (KEY OF FIG. 6)

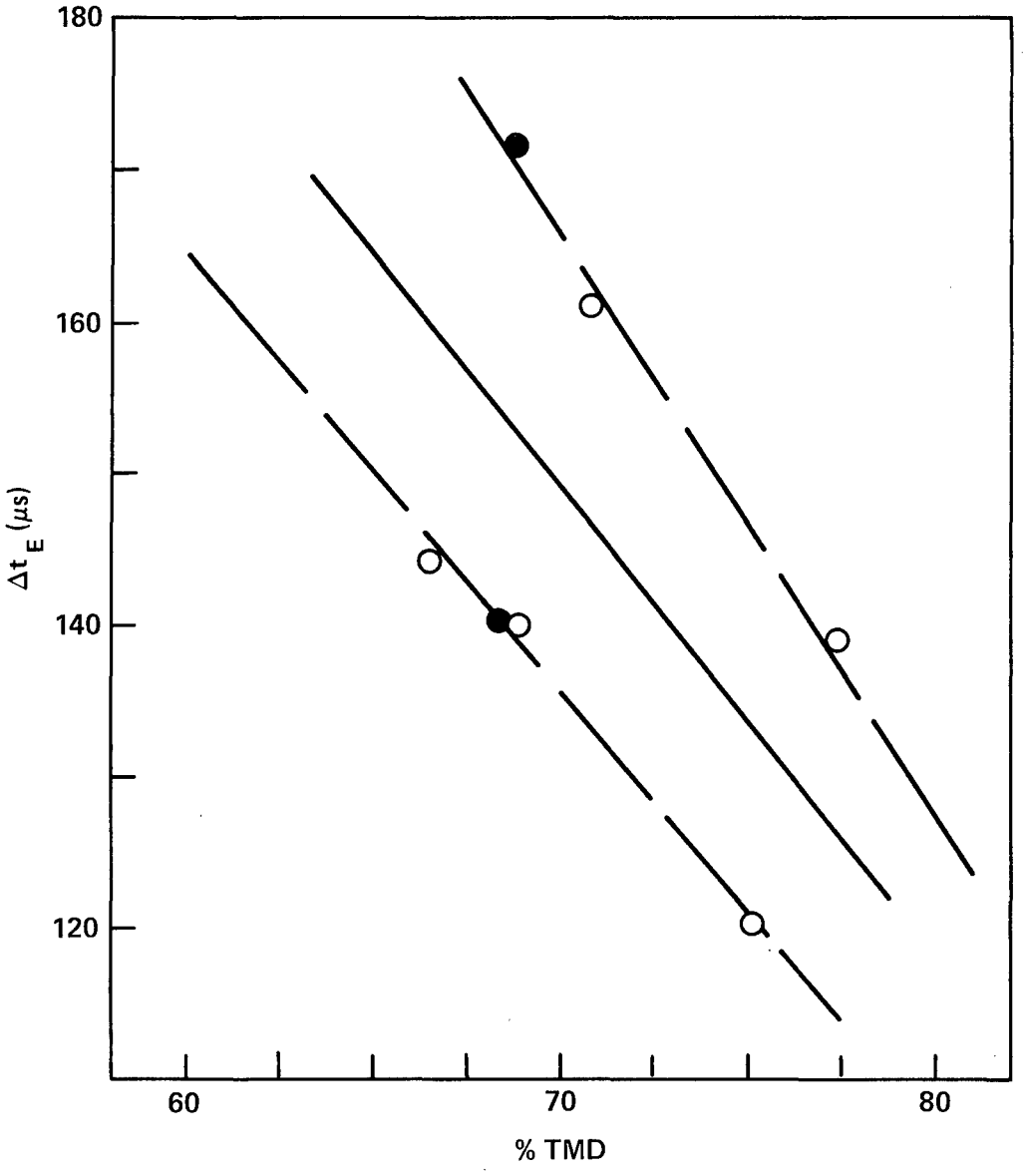

FIGURE 8 VARIATION OF Δt_E VS % TMD FOR 67μ - AND 115μ - PA
(○ 67μ PA, ● 115μ PA)

90-110°C and 120-180 atm. Optical observation or continuous electronic recording of electrical resistance or both could clarify such events in the transitional region. Similarly, the ambiguity of Shot 1504 here and of Shot 811 in Reference (1) occurred in low pressure regions and could be resolved by the proposed instrumentation. Consequently we have used a tube strong enough to contain the low pressure reactions and probe instrumentation as well as sufficiently transparent for optical observations. This system has been designed and is being developed by H. W. Sandusky. It will be used to supplement information obtained by use of the regular DDT tube, and PA will be the first explosive studied.

IV. SUMMARY AND CONCLUSIONS

1. Ground tetryl exhibits DDT behavior that appears to conform to the physical model proposed for 91/9 RDX/wax.

2. Its ℓ vs. %TMD curve is U shaped and lies between the curves for fine and coarse tetryl except at the higher porosities (%TMD $\leq$ 64) where it appears to cross the curve for fine tetryl.

3. Particle size distribution, most inadequately described by $\bar{\delta}$, can have profound effects on the DDT behavior. In the case of tetryl, grinding has eliminated any evidence of the variant mechanism of the transition as well as changed the shape and location of the ℓ vs. %TMD curve.

4. Curves of Δt_D vs. %TMD for fine and coarse tetryl are also U shaped with minima near the %TMD at which the minima of the ℓ vs. %TMD curves occur. The values are 69% and 73.5% TMD for the fine and coarse tetryl, respectively.

5. Picric acid also has a U shaped ℓ vs. %TMD curve which lies very close to the corresponding curve for fine tetryl from 78% down to 65% TMD where the two curves intersect.

6. PA has a much longer relative time to detonation Δt_D at 70% TMD than any of the other explosives that have been studied in our apparatus.

7. The interval Δt_D is made up of (1) Δt_P, the time between the formation of the (first) convective flame front and the formation of the (first compressive) PC front and (2) Δt_E, the time between the formation of the PC compression front and the onset of detonation. (Here all three Δts must be referred to the time of discharge of the same IP.) The interval Δt_E for picric acid is normal in size. Hence it is the earlier interval Δt_P which is responsible for the large Δt_D observed.

8. These observations confirm that it is the difficult ignition and propagation of combustion which is responsible for PA's uncommonly large value of Δt_D.

9. The difference in ℓ at 70% TMD for PA (67μ) and the narrow sieve fraction, PA (115μ), is about the maximum to be expected from the precision of the data. Hence, no significant difference has been established at this degree of compaction.

REFERENCES

1. Price, D., Bernecker, R. R., Erkman, J. O., and Clairmont, A. R., "DDT Behavior of Tetryl and Picric Acid," NSWC/WOL TR 76-31, 21 May 1976.

2. Bernecker, R. R., and Price, D., Combustion and Flame Vol. 22, 119-129 and 161-170 (1974). See also NOLTR 72-202.

3. Price, D., and Bernecker, R. R., "DDT Behavior of Waxed Mixtures of RDX, HMX, and Tetryl," NSWC/WOL TR 77-96, 18 Oct 1977.

4. Korotkov, A. I., Sulimov, A. A., Obmenin, A. V., Dubovitskii, V. F., and Kurkin, A. I., "Transition from Combustion to Detonation in Porous Explosives," Combustion, Explosion, and Shock Waves, Vol. 5, 216-222 (1969).

5. Fogel'zang, A. E., Margolin, A. D., Kolyasov, S. M., and Khasyanov, Kh. Zh., "Combustion of Picric Acid" ibid., Vol. 11 No. 6, 719-26 (1974).

Appendix A

SIEVE ANALYSIS OF GROUND TETRYL; INTERPOLATION FOR DIFFERENT PARTICLE SIZE

Table A1 presents the sieve analysis for the ground tetryl. As remarked in the text, this is the only time, of perhaps six attempts, that the Charge Preparation Group was able to sieve tetryl successfully. The difficulty arose from an electrostatic charge of the tetryl particles that resulted in their plugging the sieve openings despite the fact that the sieves were electrically grounded. Hence the data of Table A1 must be suspect in that the sieve openings might have been choked if not completely blocked. The data give an average particle size $\bar{\delta}$ of 160μ for the ground tetryl.

As much as possible of our work on pure HE is carried out at $\bar{\delta}$ = 115μ (a narrow cut between sieves of 105 and 125μ openings). Since we do not have values for tetryl at this $\bar{\delta}$ and were unsuccessful in obtaining the sieve cut, it would be convenient to have some method of interpolation. This has been done as follows.

Comparisons are generally made at 70% TMD. Hence from Figure 3 at 70% TMD, we read the $\bar{\delta}$ vs. ℓ values of Table A2. Then

$$s = 470/\bar{\delta}$$

is computed. As s is directly proportional to $\bar{\delta}^{-1}$, it is also proportional to the surface/volume ratio of the particle and to the total particle surface area per unit volume in the bed. For the data of Table A2 neither ℓ vs. $\bar{\delta}$ nor ℓ vs. s is linear, but ℓ vs. log s is (see Figure A1). By interpolation, the predetonation column length for 70% TMD tetryl ($\bar{\delta}$ = 115μ) is 116 mm.

Obviously, the curve for ground tetryl in Figure 3 has not been well established (large scatter in the data), and the assumption that $\bar{\delta} \curvearrowright$ 160μ for the ground tetryl is open to some question. Consequently the approximation is considered just that and nothing more.

Table A1

SIEVE ANALYSIS OF GROUND TETRYL (844)

Sieve No.	Sieve Opening (μ)	Wt. (gm) Retained on Sieve	% Wt.	Cum. Wt. %
20	850	0.0		
30	600	0.0		
40	425	0.2	0.1	100.0
50	300	9.4	5.1	99.9
70	212	45.3	24.6	94.8
100	150	45.8	24.9	70.2
140	106	49.8	27.0	45.3
200	75	31.4	17.1	18.3
270	53	0.9	0.5	1.2
325	45	0.8	0.4	0.7
Pan		0.6	0.3	0.3

Table A2

DATA USED FOR INTERPOLATION OF ℓ vs. $\bar{\delta}$

$\bar{\delta}(\mu)$	ℓ(mm)	$s(\mu^{-1})$*	
20	184	23.50	
160	103	2.94	
470	63	1.00	
115	116	4.09	Interpolation

*$s = 470\ \delta^{-1}$

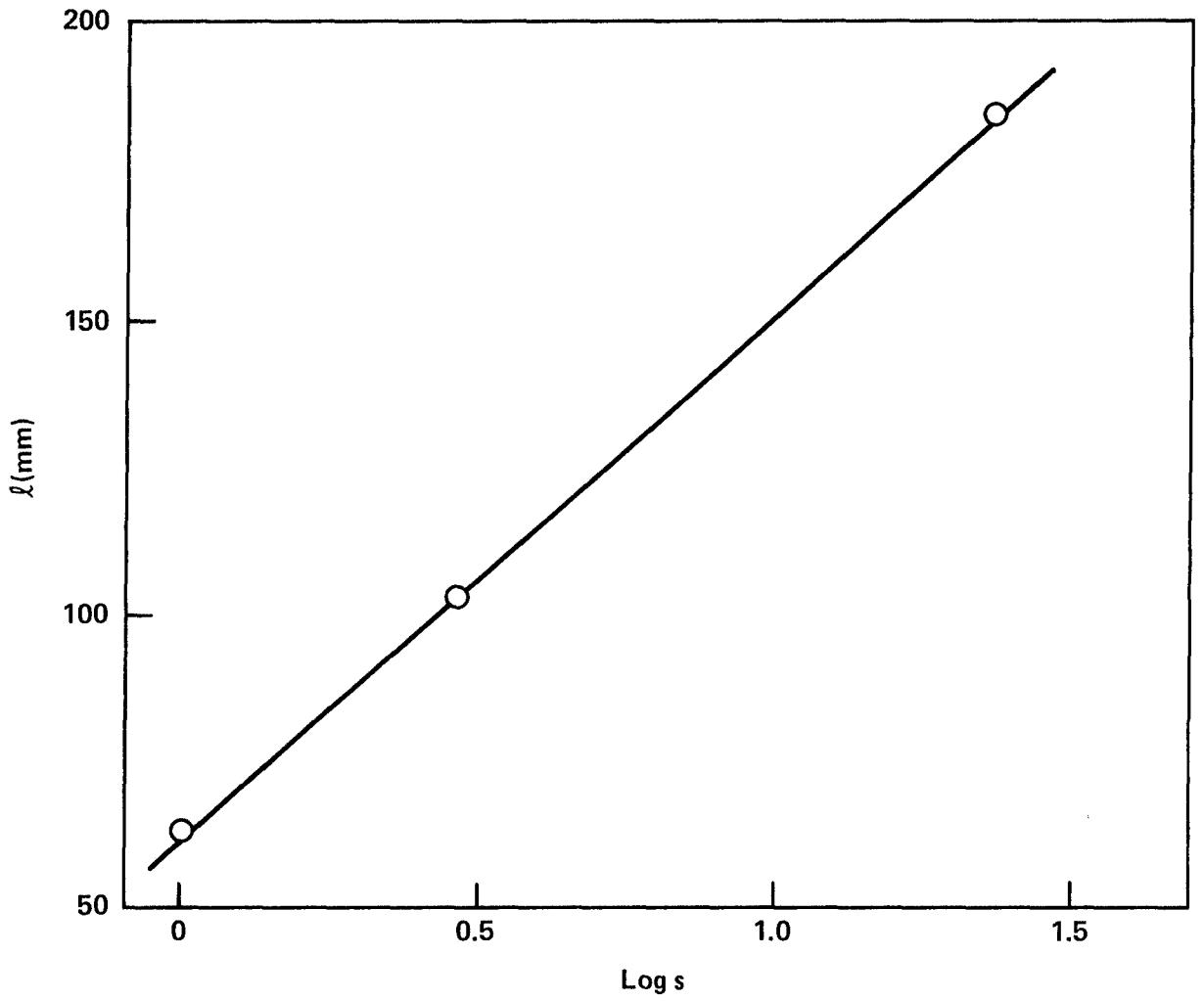

FIGURE A1 VARIATION OF ℓ WITH Log s FOR 70% TMD TETRYL

Appendix B

DETAILED DATA FOR GROUND TETRYL

Detailed data from the shots on ground tetryl are given in Table B1. The records are shown in Figures B1-9. Shots 1015, 1313, 1113, 1512, and 1112 (Figures B1, 2, 4, 5, and 8) have records indicating a DDT mechanism following the original physical model[2]. Shot 615 (Figure B7) has records suggesting the behavior of the fine and the coarse tetryls[1]. The remaining three sets of records give no evidence about the transition mechanism with the possible exception of 1307 (Figure B9).

The shot on 61% TMD ground tetryl (Figure B9) is unusual on two counts: velocity of the PC wave and rearward travelling compression. The first detected compressive wave travels at 0.4 mm/μs, lower by a factor of two or more than the PC wave velocities measured in all three tetryl series. Hence it suggests the possibility of a variant behavior with the explosive event at about x = 170 mm, very near ℓ(182 mm). This might be the case despite the sharpening of the pressure fronts shown in Figure B9b; on the other hand, the path of the PC wave could have been drawn more steeply (velocity ↶ 0.6 mm/μs) and acceleration could have occurred in the unmonitored interval just before the point of detonation onset.

Finally the rearward reflection here has a velocity of 6.2 mm/μs, about 12% greater than the measured detonation velocity. However, like Shot 1402 on 77% PA, the ignitor bolt showed no dent and that end of the DDT tube was not in small fragments. For both shots, this rearward wave is considered a shock, not a retonation.

Table B1

DETAILED DATA FOR TETRYL 844

Shot No.	1015		1313		614		1113	
Density								
g/cm^3	1.553		1.513		1.464		1.402	
% TMD	89.8		87.5		84.6		81.0	
IP Data	x̄	t̄	x̄	t̄	x̄	t̄	x̄	t̄
	41.4	0.0*	40.8	0.0*	41.4	0.0*	41.4	0,2.7*
	60.7	38.0*	59.8	26.2*	54.2	11.8*	60.6	5.05*
	79.8	61.8*	78.9	48.5*	79.6	36.7*	79.6	33.95*
	105.2	92.85*	104.4	76.3*	104.9	56.6*	105.0	63.0*
	124.1	121.6*	129.7	99.3*	130.3	67.4*	117.7	76.7
	143.3	-	155.2	122.55*	155.8	70.8	130.4	90.8
	162.3	165.1[a]	180.6	143.5	181.2	74.0	155.8	97.95
	181.4	179.3[a]	206.0	163.0	206.6	78.0	181.2	101.7
	206.8	-	225.0	172.55	232.0	81.6	206.6	105.7
	232.2	274.5[a]	244.1	174.7	257.4	84.3	257.4	113.1
	263.9	296.75	263.1	177.5				
SG Data	x̄	t̄	x̄	t̄	x̄	t̄	x̄	t̄
	20.4	161.1,184.5	20.6	90.2	20.8	-	20.8	38.7
	67.3	149.5,167	92.3	46.9,123.4	49.5	-	67.1	64.8
	92.7	170,194	143.3	98.7,145.6	74.7	21.5	117.9	60,81.9
	118.0	203	193.9	143.3,164.3	105.2	52.5	143.3	89.7
	143.5	221	231.9	-	143.0	-		
ℓ, mm	F		225^{+4}_{-2}		120^{+2}_{-3}		146 ± 3	
D, mm/μs	F		7.65 ± 0.59		7.5		7.2	

a. IP records ambiguous; values judged best assignment
*Custom-made probe
All x in mm, t in μs. F means failure.

Table B1 (Cont.)

DETAILED DATA FOR TETRYL 844

Shot No.	1512		1114		615		1112	
Density g/cm^3	1.324		1.324		1.284		1.133	
% TMD	76.5		76.5		74.2		65.5	
IP Data	x	t	x	t	x	t	x	t
	41.5	0.0*	41.7	0.0**	28.80	6.5*	54.2	0.0*
	54.2	60.6*	60.7	22.0*	41.65	0.0*	73.4	37.8*
	66.9	82.3*	79.9	34.6*	54.35	5.0	92.5	98.4*
	79.6	103.0*	92.5	36.7*	67.05	60.5	117.9	190.9*
	92.3	121.7	105.3	38.5*	79.75	76.7	143.3	263.2*
	105.0	138.3	117.9	40.1*	105.15	105.7	168.5	287.0*
	130.4	168.35	130.6	43.4*	130.55	110.2	194.1	292.8*
	155.8	175.4	156.0	46.7*	155.95	114.0	219.5	296.9*
	206.6	182.95	181.4	50.25*	181.35	118.3	244.9	300.65*
	257.6	189.75	206.8	54.6*	257.55	129.8	264.0	304.2*
			257.6	61.9*				
SG Data	x	t	x	t	x	t	x	t
	20.6	-	20.6	-,56.6?	20.7	-	20.7	-
	54.4	-	67.1	12.9,37.4	41.7	-,95	79.9	207.4
	73.4	114.0,141.3	92.3	-	60.8	32,84	105.3	236.5
	92.3	-,150.7	117.7	-	79.9	60,95	130.6	250.3
	111.5	125,141.3, 164.3	136.8	-	98.8	80,-	155.7	262.6
ℓ, mm	145±2		78±2		115±2		168±3	
D, mm/μs	7.1		6.5		6.5		5.6	

*Custom-made probe
** Commercial probe, in circuit designed for response at high resistance
All x in mm, t in μs. F means failure.

Table B1 (Cont.)

DETAILED DATA FOR TETRYL 844

Shot No. 1307

Density
g/cm^3 1.056
% TMD 61.0

IP Data x	t
54.4	0.0*
73.4	84.2*
92.5	150.9*
111.5	204.2*
130.6	250.1*
156.0	300.75*
181.4	327.0*
206.9	331.85*
232.2	336.6*
257.6	340.85*

SG Data x	t
20.3	355
79.6	102,340-347
105.0	145,332-343
130.3	223,336-340
155.8	268,326-334

ℓ, mm 182±2

D, mm/μs 5.5

*Custom-made probe
All x in mm, t in μs. F means failure.

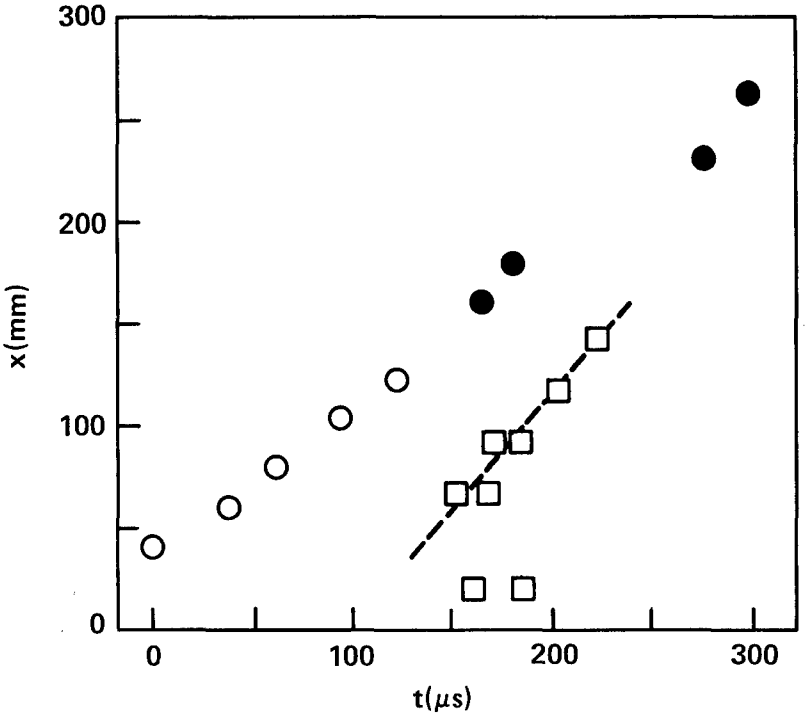

a. DISTANCE-TIME DATA (○ WOL PROBES, ● COMMERCIAL PROBES, □ SG EXCURSION TIMES)

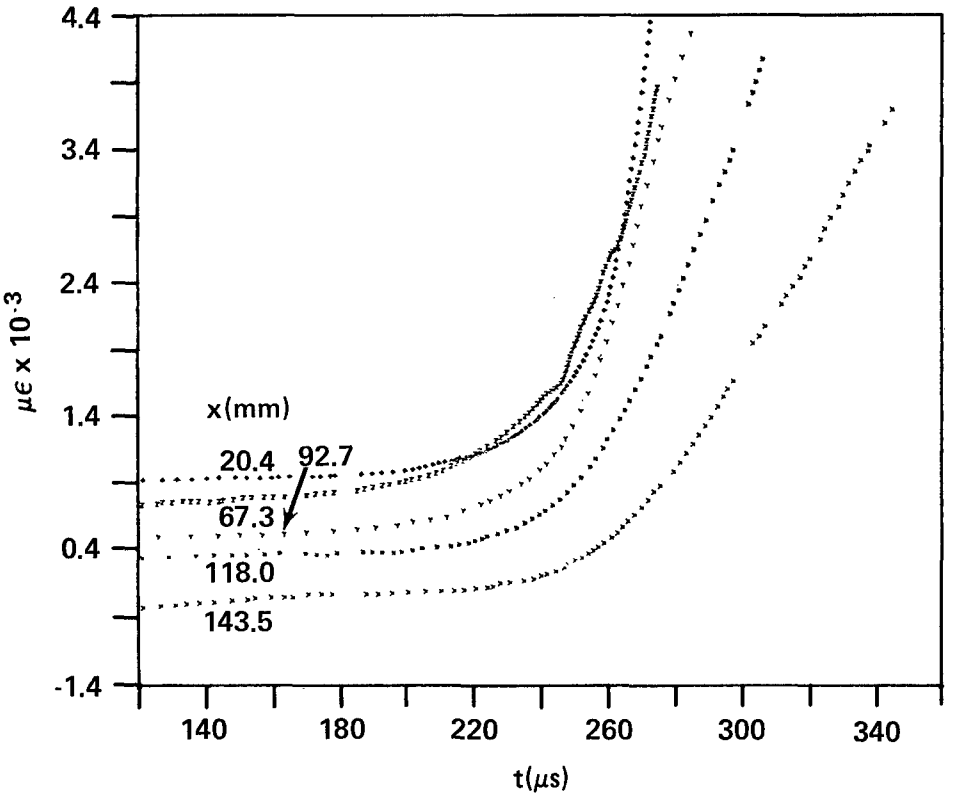

b. STRAIN-TIME DATA. EACH CURVE, EXCEPT THE LOWEST HAS BEEN RAISED 200 $\mu\epsilon$ (OR AN INTEGRAL MULTIPLE THEREOF) FOR BETTER DATA DISPLAY

FIGURE B1 SHOT 1015 ON 89.8% TMD GROUND TETRYL, ρ_o=1.55 g/cm^3

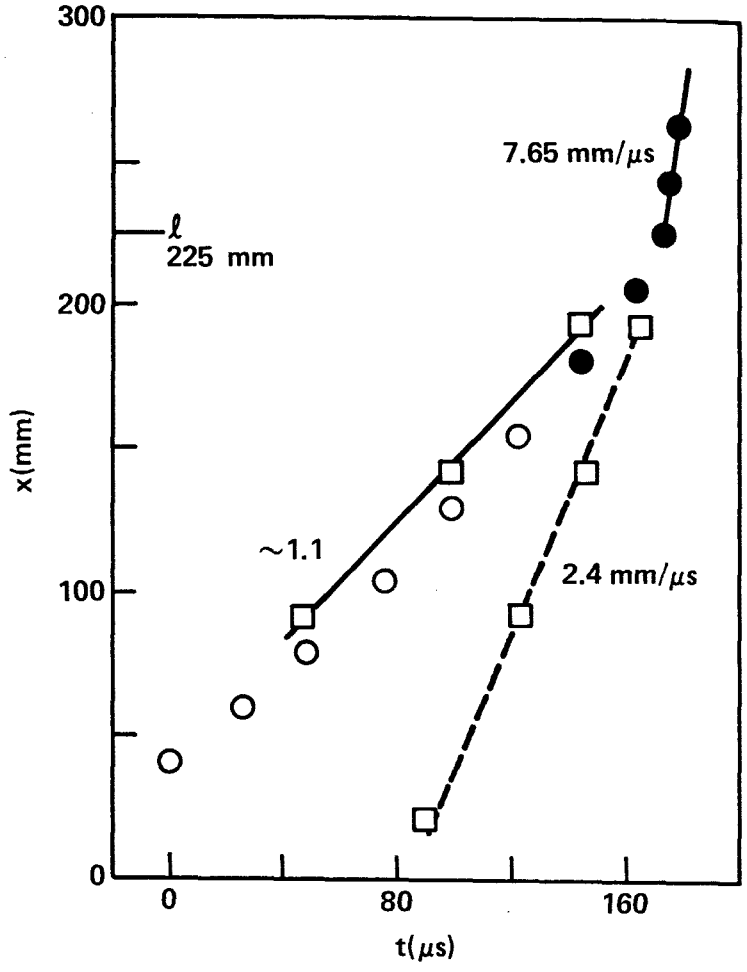

a. DISTANCE-TIME DATA (KEY OF FIG. B1a)

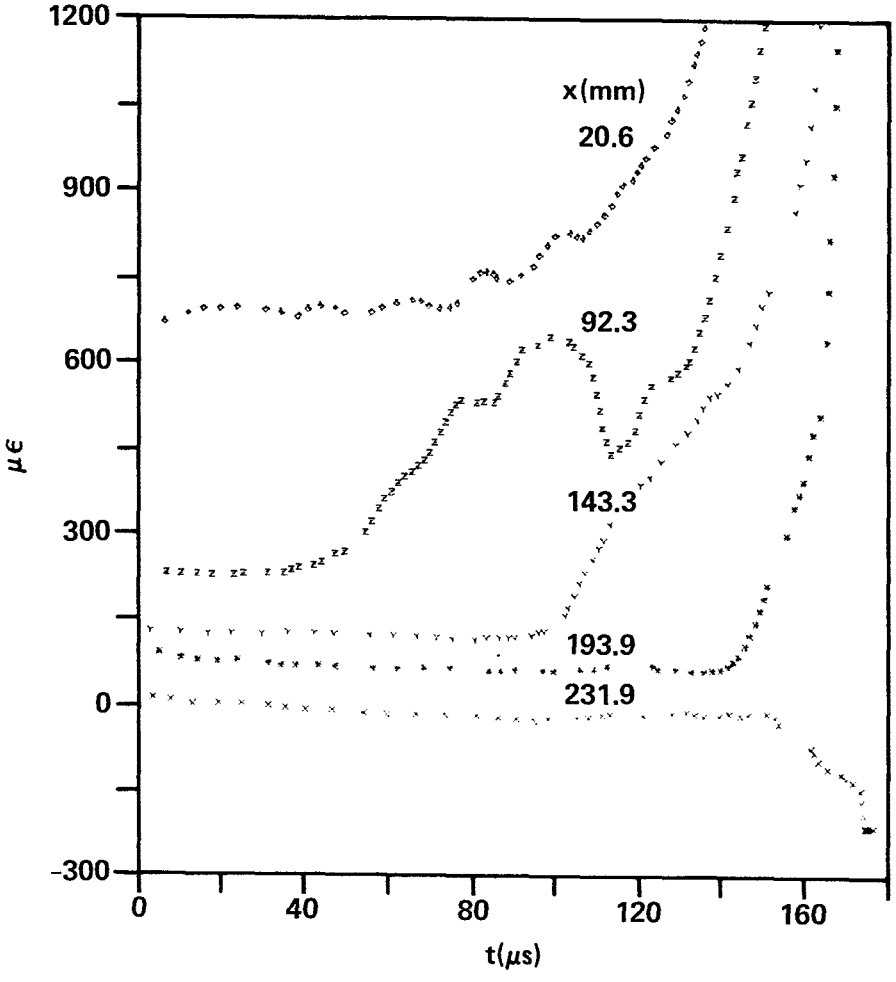

b. STRAIN-TIME DATA (KEY OF FIG. B1b WITH INCREMENT 75με)

FIGURE B2 SHOT 1313 ON 87.5% TMD GROUND TETRYL, ρ_o=1.51 g/cm^3

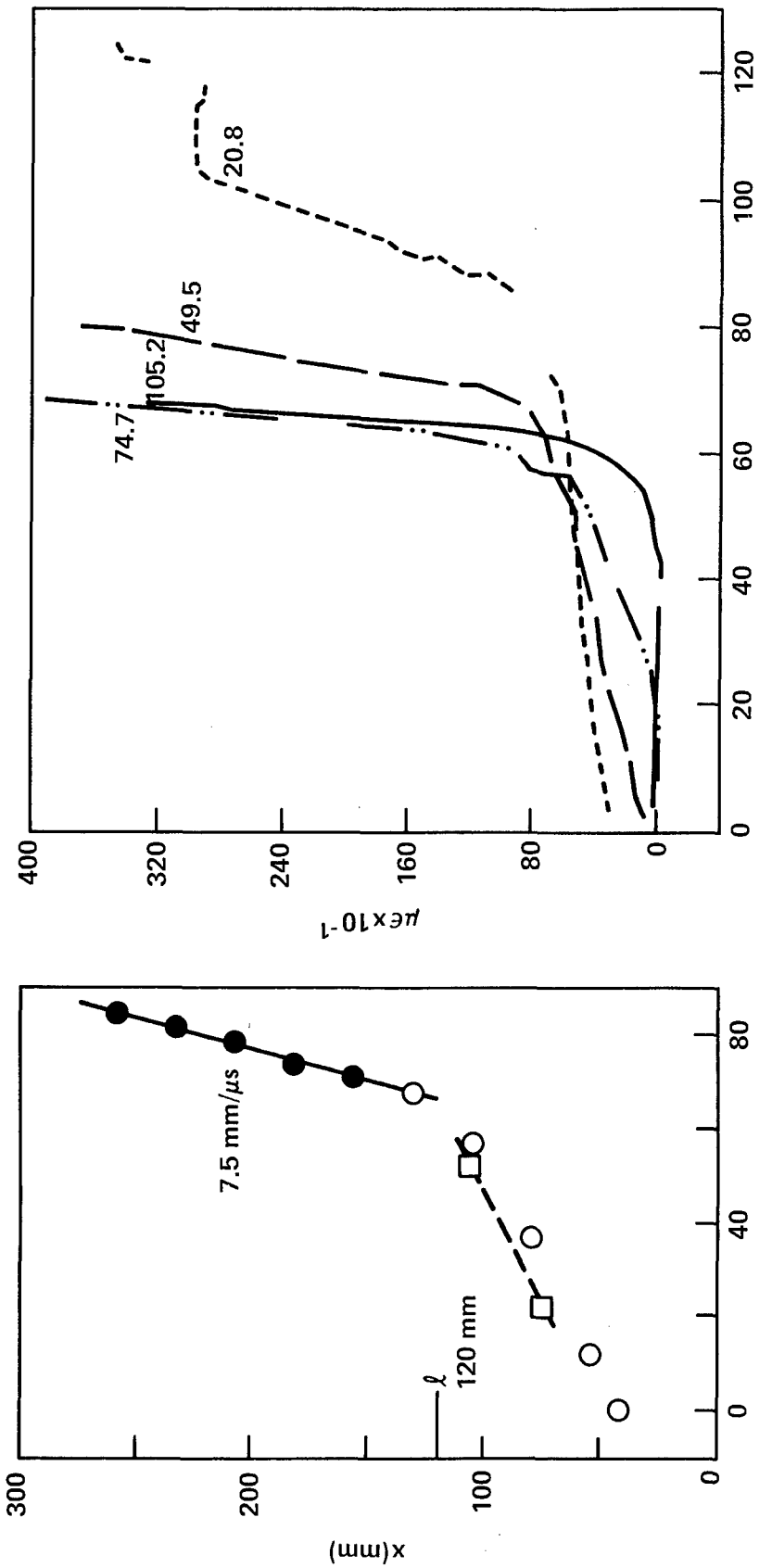

a. DISTANCE-TIME DATA (KEY OF FIG. B1a)

b. STRAIN-TIME DATA

FIGURE B3 SHOT 614 ON 84.6% TMD GROUND TETRYL, ρ_o=1.46 g/cm^3

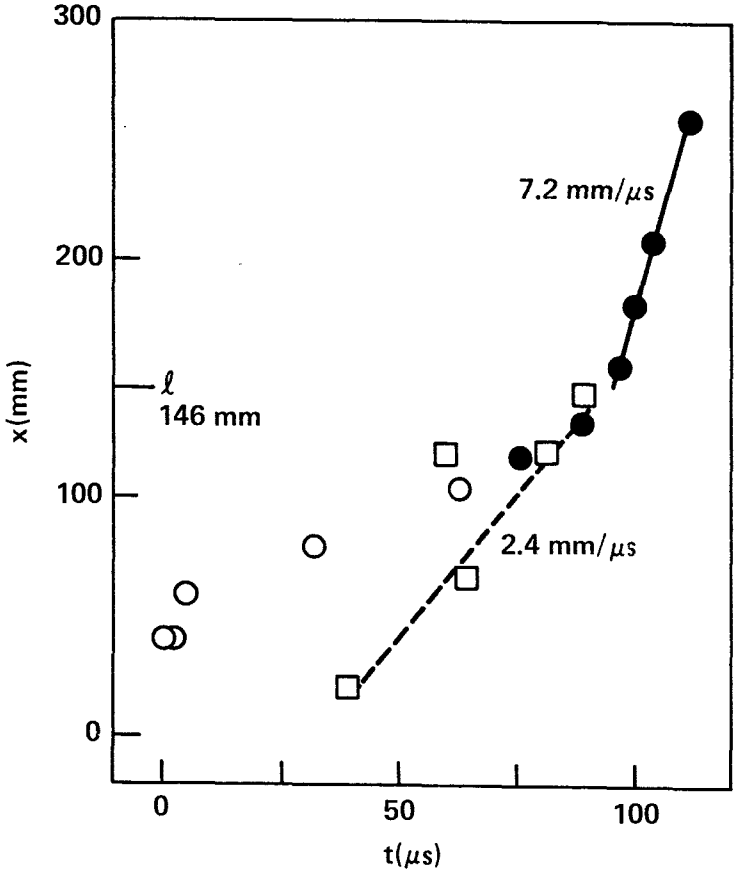

a. DISTANCE-TIME DATA (KEY OF FIG. B1a)

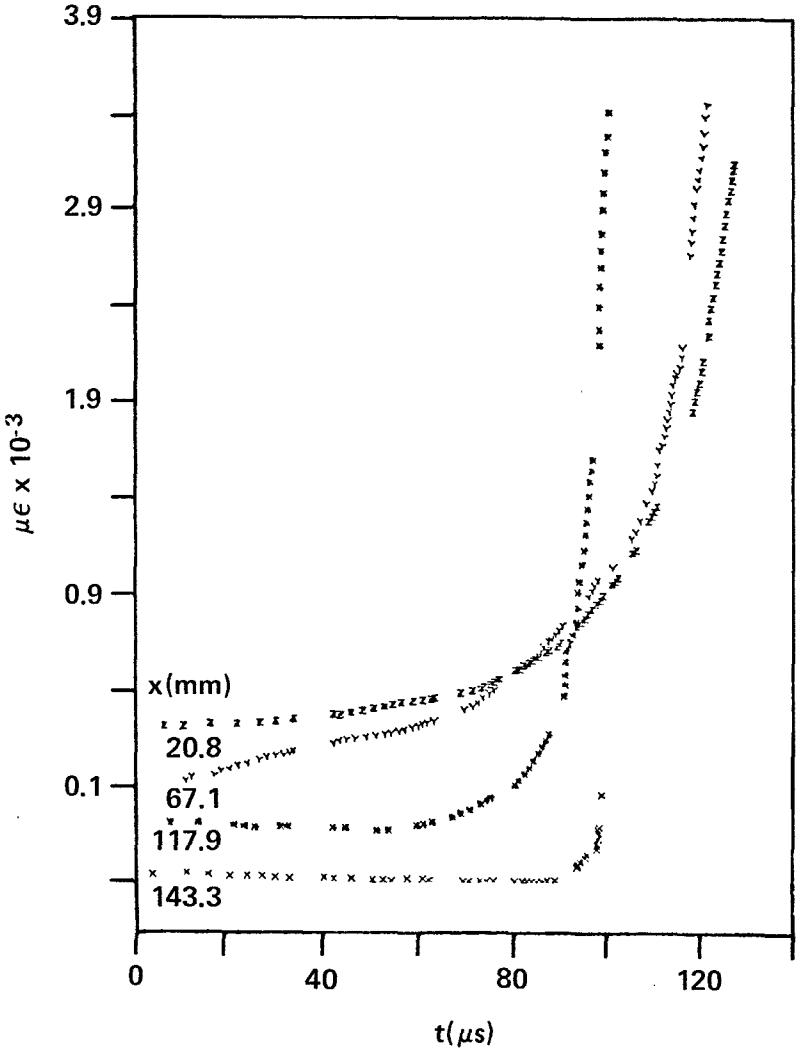

b. STRAIN-TIME DATA (KEY OF FIG. B1b)

FIGURE B4 SHOT 1113 ON 81.0% TMD GROUND TETRYL, ρ_o=1.40 g/cm^3

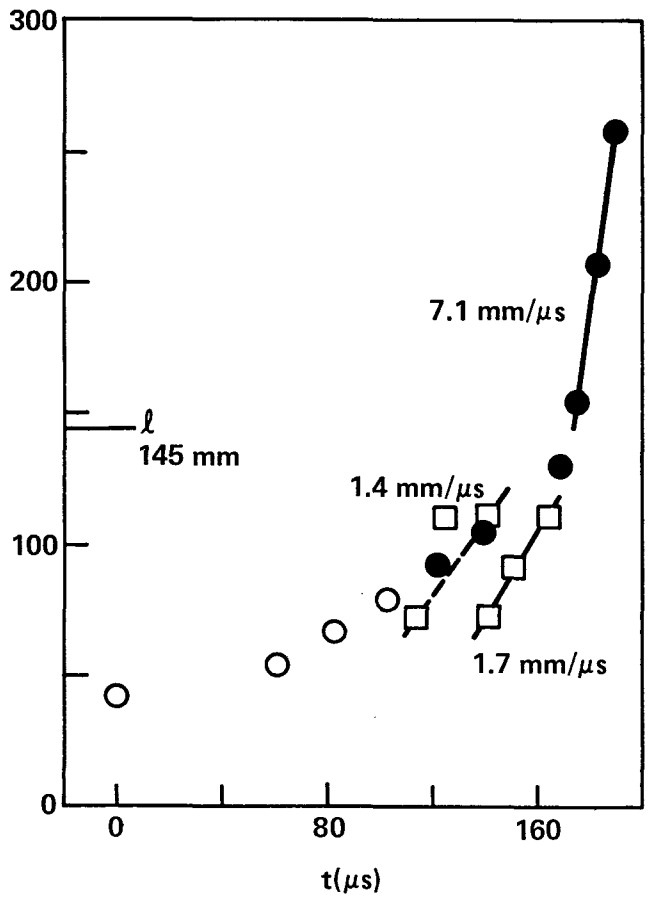

a. DISTANCE-TIME DATA (KEY OF FIG. B1a)

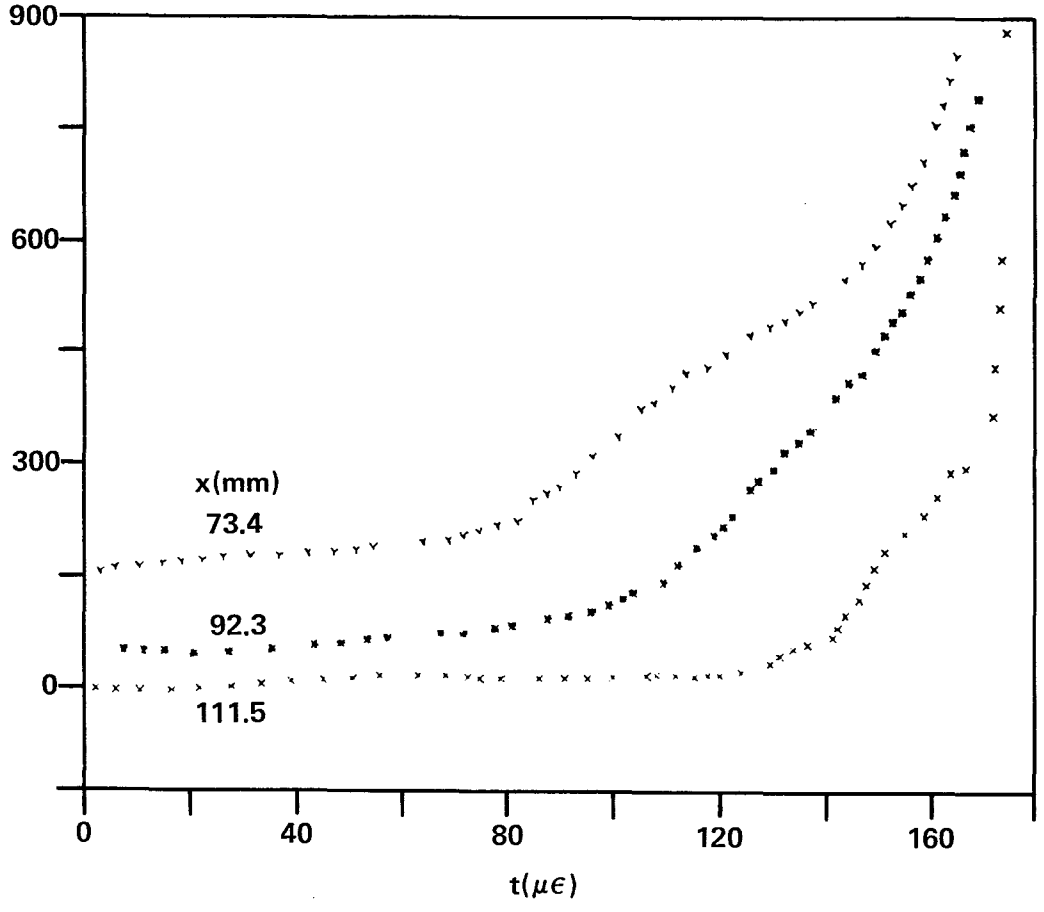

b. STRAIN-TIME DATA (KEY OF FIG. B 2b)

FIGURE B5 SHOT 1512 ON 76.5% TMD GROUND TETRYL, ρ_o=1.32 g/cm^3

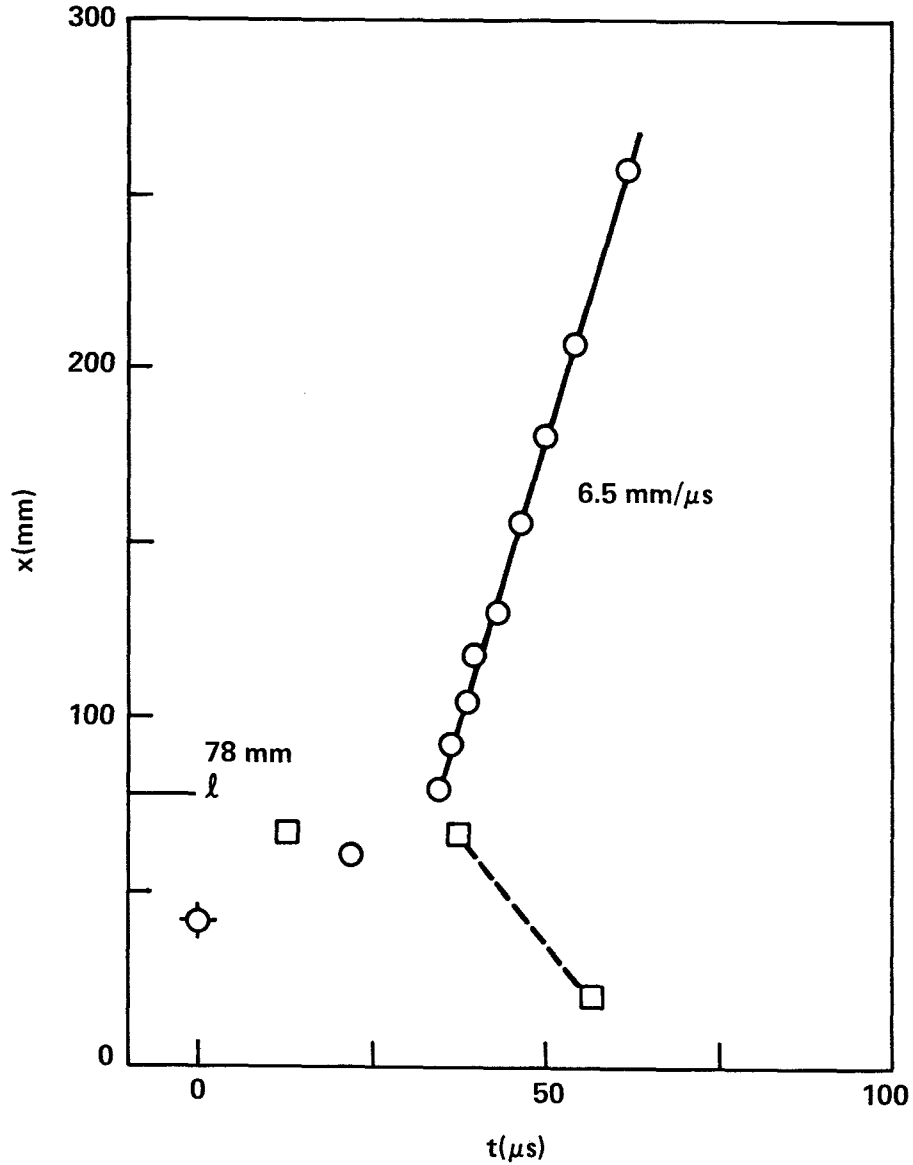

a. DISTANCE-TIME DATA. (⊖ COMMERCIAL PROBE IN CIRCUIT DESIGNED FOR RESPONSE AT HIGH RESISTANCE AND KEY OF FIG. B1a)

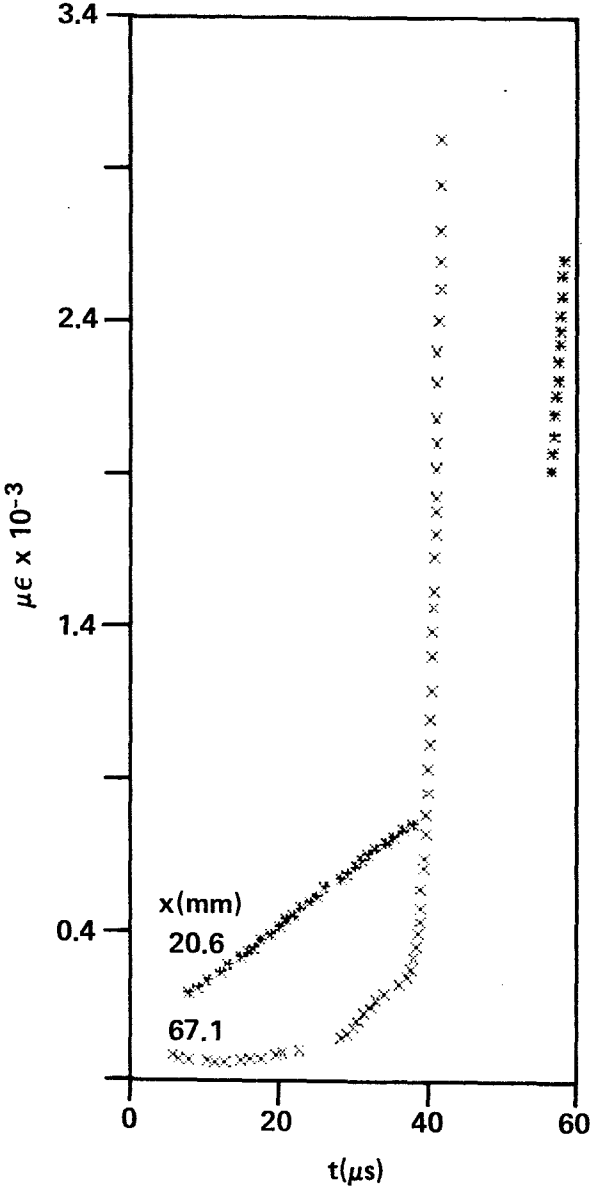

b. STRAIN-TIME DATA

FIGURE B6 SHOT 1114 ON 76.5% TMD GROUND TETRYL, ρ_o=1.32 g/cm^3

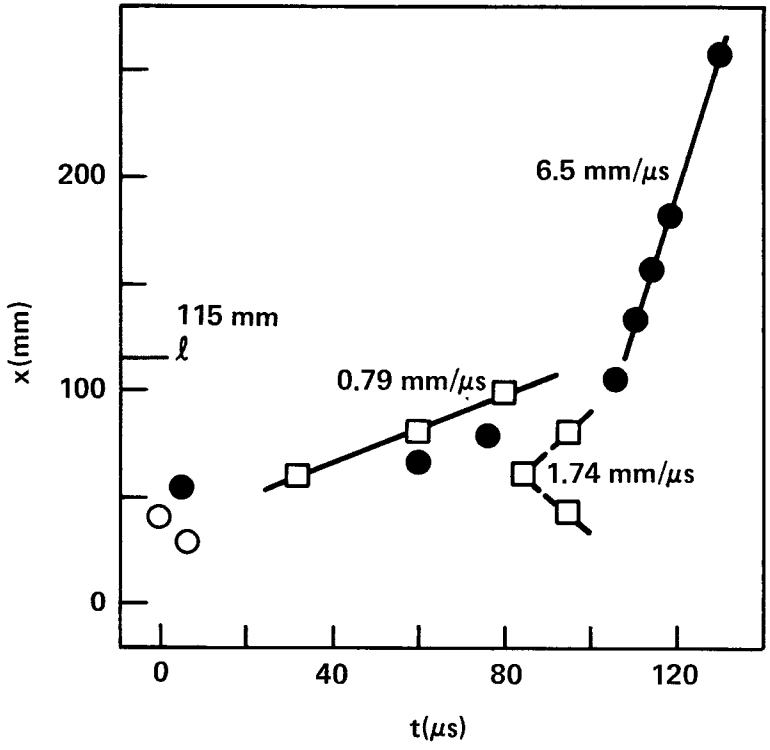

a. DISTANCE-TIME DATA (KEY OF FIG. B1a)

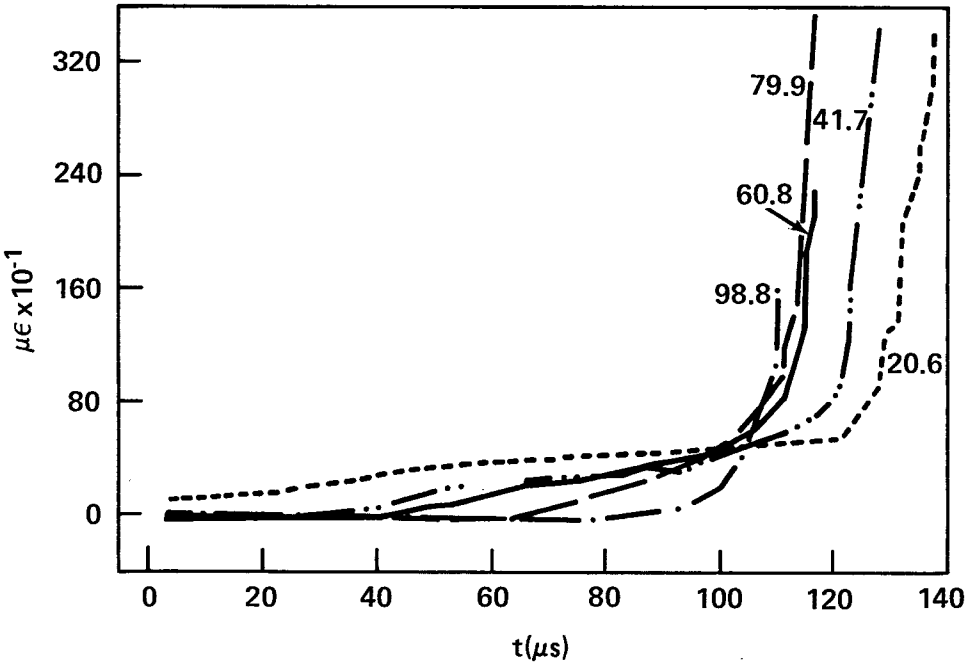

b. STRAIN-TIME DATA

FIGURE B7 SHOT 615 ON 74.2% TMD GROUND TETRYL, ρ_o =1.28 g/cm^3

Appendix C

DETAILED DATA FOR PICRIC ACID

The data for the final shots with PA are given in Table C1 and plotted in Figures C1-C5. Since each result had to be considered in drawing conclusions about the PA series, these data have been discussed in the main text.

Table C1

DETAILED DATA FOR PICRIC ACID

Shot No.	1402		1514[b]		1504		1407[c]	
Density g/cm^3	1.362		1.104		1.090		1.203	
%TMD[a]	77.4		62.7		61.9		68.4	
IP Data	x̄	t̄	x̄	t̄	x̄	t̄	x̄	t̄
	41.5	0.0*	41.7	0.0	41.9	-d	41.5	0.0*
	79.8	131.5*	79.8	261.3*	54.6	0.0*	60.6	13.85*
	105.2	198.85*	130.6	575.0[d]	80.0	127.5*	79.6	57.2*
	130.6	273.6*	168.7	1096.4*	105.4	266.4*	105.0	122.7*
	149.6	303.4*	206.9	1170.0*	130.8	417.0*	130.3	185.4*
	168.7	315.8*	245.0	1859.3*	156.2	465.4*	149.5	228.6*
	187.7	328.5*	270.3	1887.9*	175.4	670.8*	168.5	272.6
	206.8	334.5*	295.7	1892.8*	194.4	910.7	187.6	315.6
	225.8	337.5*	321.2	1897.5	213.5	1473.0	206.6	345.4
	244.9	340.6*	346.6	1902.4	238.9	-	232.0	363.1
	263.9	343.7*	371.9	1907.5	264.3	-	263.8	368.2
SG Data	x̄	t̄	x̄	t̄	x̄	t̄	x̄	t̄
	20.6	175,359-372			20.4	all pressures	20.6	277
	79.5	231, -	no SG used		79.8	<0.35	67.1	250,377
	117.7	267,345	on this		117.7	kbar	92.3	255,392
	149.4	296,339	shot.		149.5	for first	117.9	271,387
	181.2	318,335			181.2	1780 μs	136.8	286,381
ℓ(mm)	196±3		279±3[b]		[242±6][e]		229^{+3}_{-0}	
D(mm/μs)	6.20		5.21		F		5.6	
σ(mm/μs)	0.03		0.05		-		-	

*Custom-made probe.
a) ρ_v = 1.76 g/cm^3. b) 18 in. tube i.e., 410 mm column of explosive. c) Sieve cut with 105 and 125μ openings; $\bar{\delta}$ = 115μ. d) Commercial probe in circuit designed for response at high resistance.
e) Tube markings. All x in mm, t in μs, F means failure.

Table C1 (Cont.)

DETAILED DATA FOR PICRIC ACID

Shot No.	1418[c]
Density g/cm^3	1.210
%TMD[a]	68.8

IP Data x	t
41.5	0.0*
67.1	97.0*
92.5	d
117.9	290.1*
143.3	407.1*
168.7	-
187.7	-
206.8	(961.6)
225.8	(964.7)
244.9	(966.85)
264.0	(970.7)

SG Data x	t
20.4	815
66.8	816
104.9	858
143.1	899
181.0	905

ℓ(mm)	192±1
D(mm/μs)	6.40
σ(mm/μs)	0.48

*Custom-made probe.
a) ρ_v = 1.76 g/cm^3.
c) Sieve cut with 105 and 125μ openings; $\bar{\delta}$ = 115μ.
d) Commercial probe in circuit designed for response at high resistance.

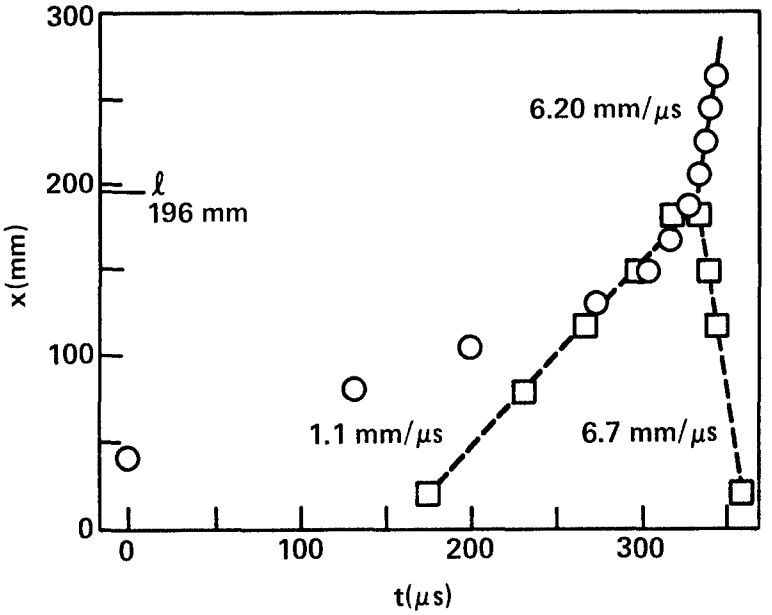

a. DISTANCE-TIME DATA (KEY OF FIG. B1a)

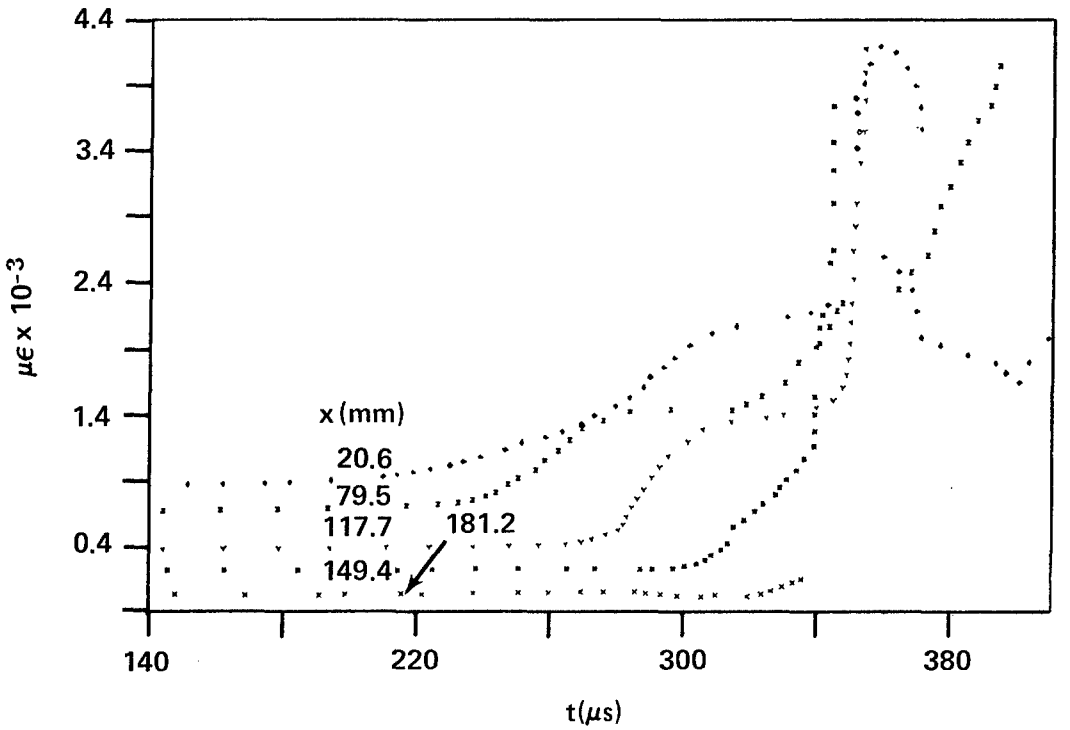

b. STRAIN-TIME DATA (KEY OF FIG. B1b)

FIGURE C1 SHOT 1402 ON 77.4% TMD PICRIC ACID (67μ), ρ_o=1.36 g/cm^3

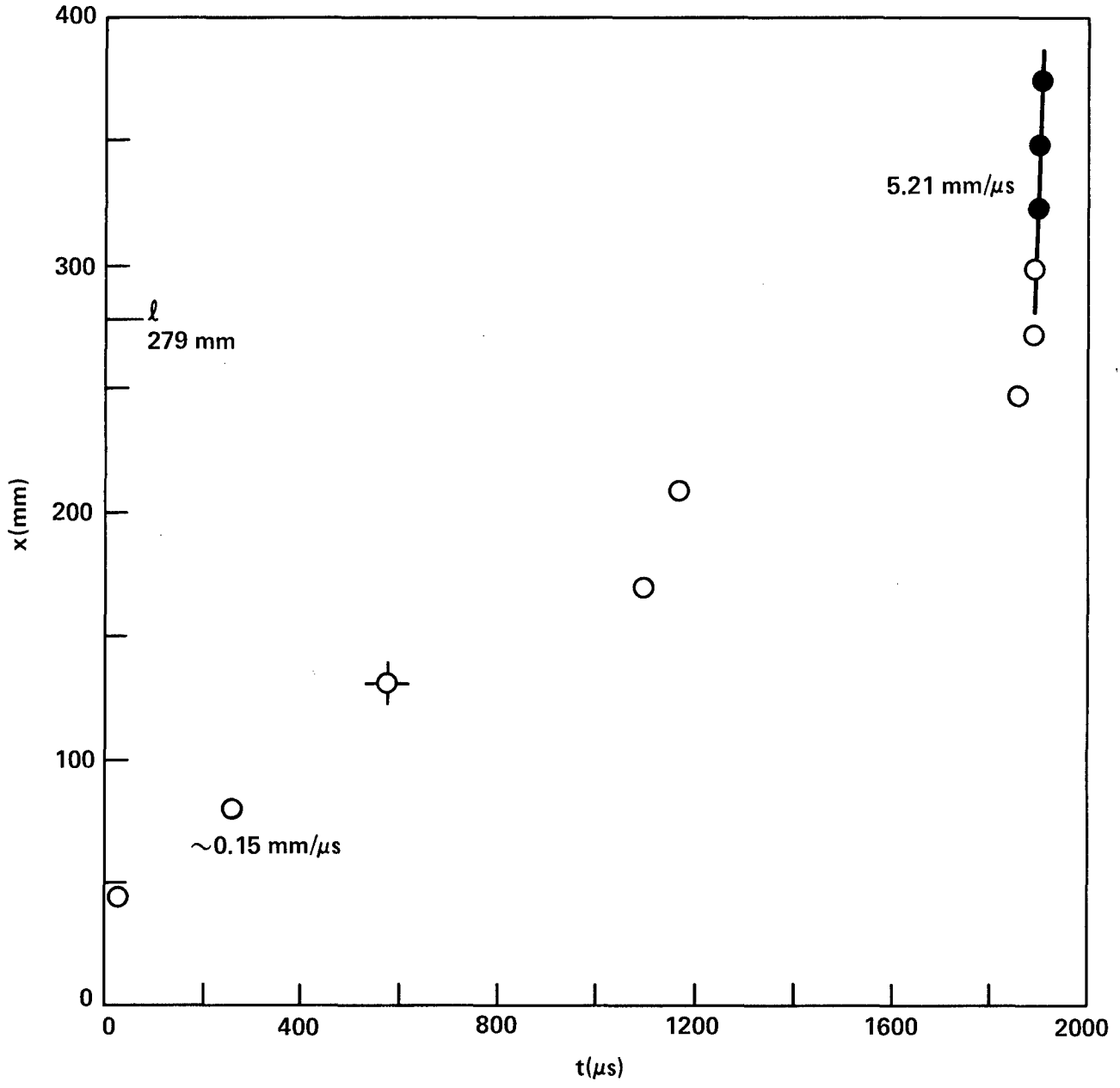

FIGURE C2 SHOT 1514 ON 62.7% TMD PICRIC ACID (67μ), ρ_o=1.10 g/cm^3
DISTANCE-TIME DATA (KEY OF FIG. B6a)

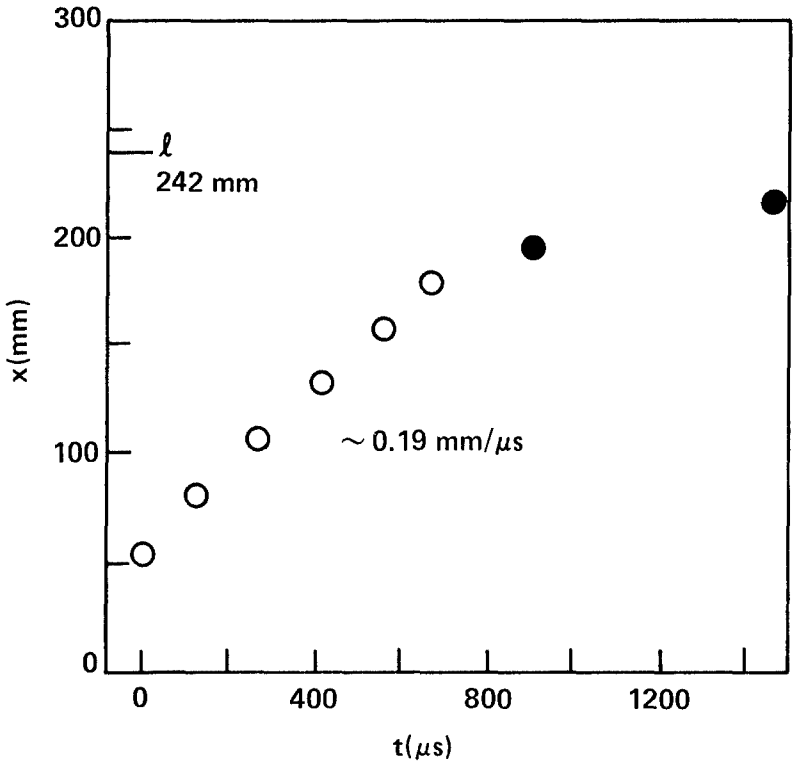

a. DISTANCE-TIME DATA (KEY OF FIG. B1a)

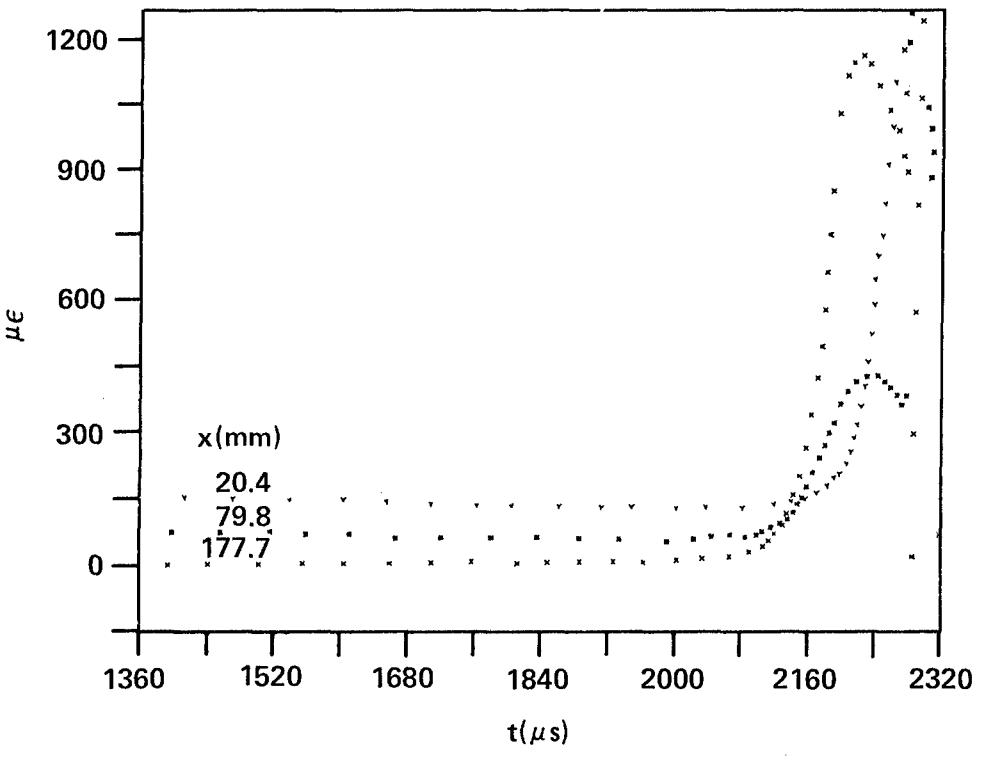

b. STRAIN-TIME DATA (KEY OF FIG. B2b)

FIGURE C3 SHOT 1504 ON 61.9% TMD PICRIC ACID (67μ), ρ_o=1.09 g/cm^3

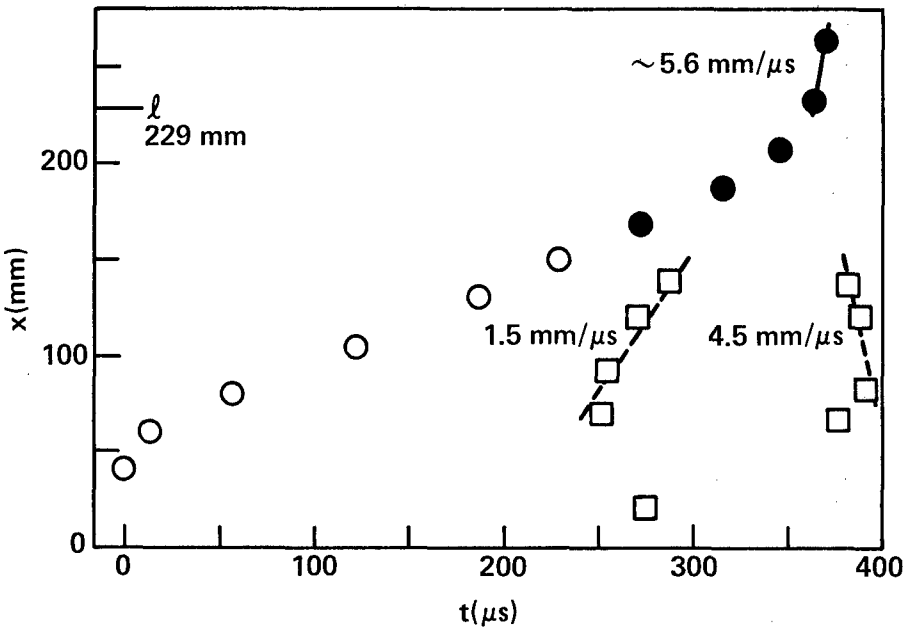

a. DISTANCE-TIME DATA (KEY OF FIG. B1a)

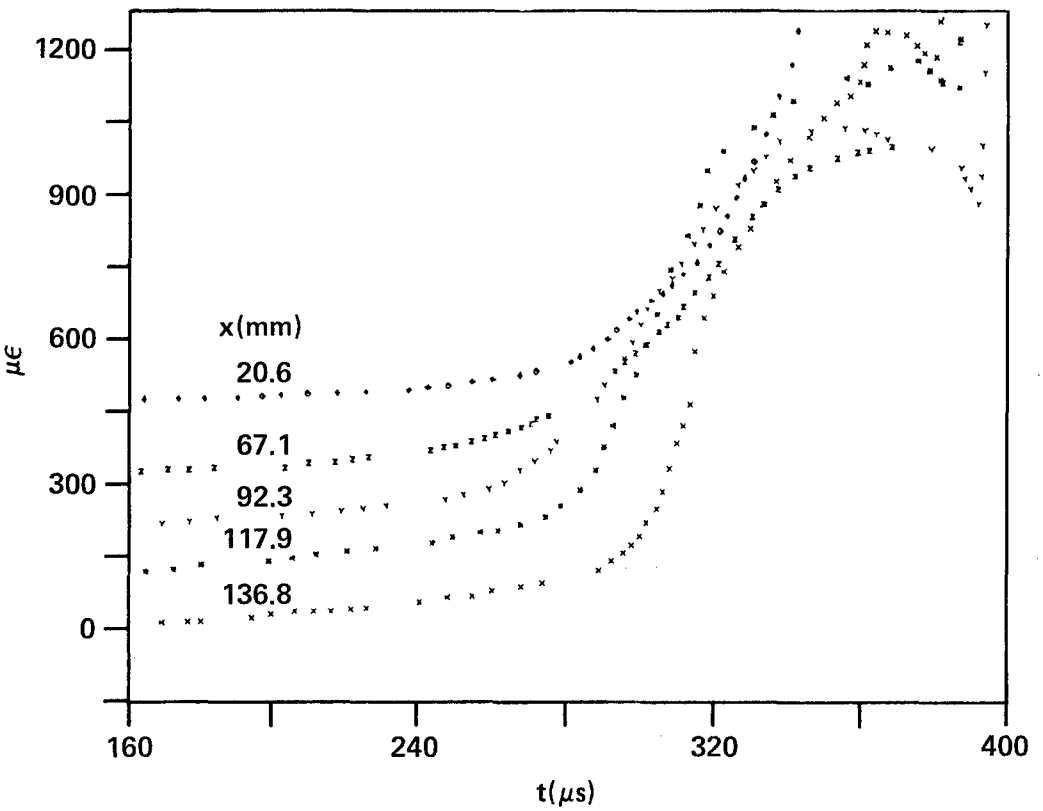

b. STRAIN-TIME DATA (KEY OF FIG. B2b)

FIGURE C4 SHOT 1407 ON 68.4% TMD PICRIC ACID (115μ), ρ_o=1.20 g/cm^3

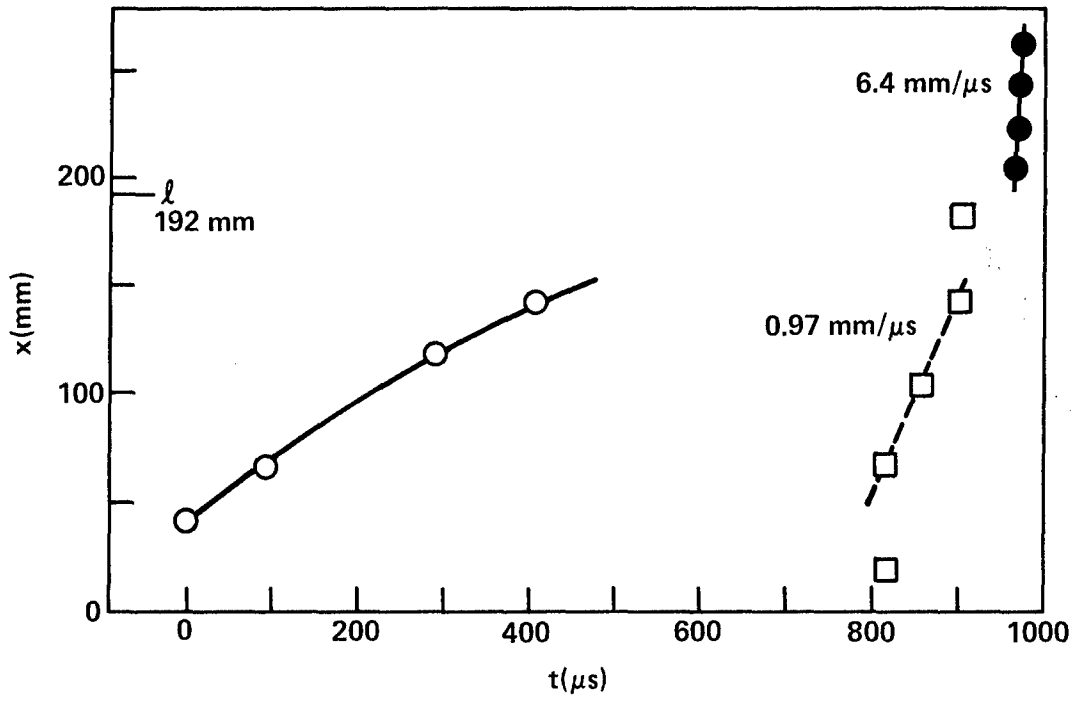

a. DISTANCE-TIME DATA (KEY OF FIG. B1a)

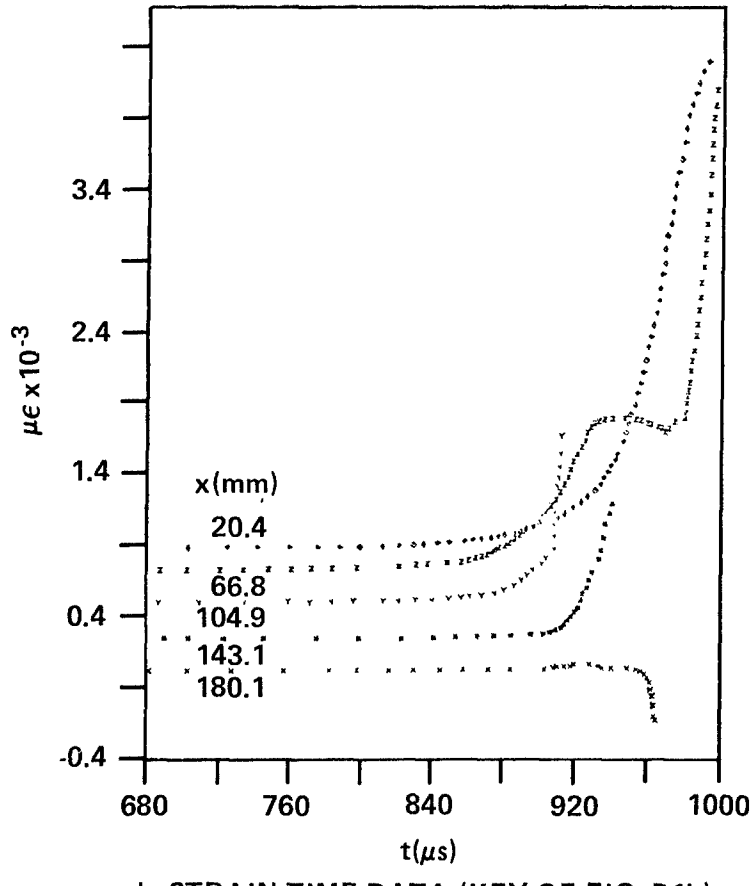

b. STRAIN-TIME DATA (KEY OF FIG. B1b)

FIGURE C5 SHOT 1418 ON 68.8% PICRIC ACID (115μ), ρ_o=1.21 g/cm^3

DISTRIBUTION LIST

	Copies
Chief of Naval Material Washington, DC 20360	
Commander Attn: AIR-350 AIR-330 Naval Air Systems Command Department of the Navy Washington, DC 20361	
Commander Attn: SEA-09G32	2
SEA-0332 SEA-0331	3
SEA-03B Naval Sea Systems Command Department of the Navy Washington, DC 20360	
Director Attn: SP-273, R. M. Kinert SP-27311, E. L. Throckmorton, Jr. Strategic Systems Project Office (PM-1) Department of the Navy Washington, DC 20376	
Office of Naval Research Attn: Rear Admiral C. O. Holmquist Technical Library (ONR-741) Department of the Navy Arlington, VA 22217	

DISTRIBUTION (Cont.)

	Copies
Commander Attn: Code 556 Technical Library H. D. Mallory Code 452 Code 5008 R. L. Derr Naval Weapons Center China Lake, CA 93555	2
Director Attn: Technical Information Section Naval Research Laboratory Washington, DC 20375	2
Office of Chief of Naval Operations Operations Evaluation Group (OP03EG) Washington, DC 20350	
Director Office of the Secretary of Defense Advanced Research Projects Agency Washington, DC 20301	
Scientific and Technical Information Facility, NASA P. O. Box 33 College Park, MD 20740	
Commanding Officer Attn: R&D Division Code 50 Naval Weapons Station Yorktown, VA 23691	
Commanding Officer Attn: Technical Library Naval Propellant Plant Indian Head, MD 20640	
Commanding Officer Attn: Information Services Naval Explosive Ordnance Disposal Facility Indian Head, MD 20640	

DISTRIBUTION (Cont.)

Copies

McDonnell Aircraft Company
Attn: M. L. Schimmel
P. O. Box 516
St. Louis, MO 63166

Commanding Officer
Naval Ammunition Depot
Crane, IN 47522

Commanding Officer
Attn: LA 151-Technical Library
Naval Underwater Systems Center
Newport, RI 02840

Commanding Officer
Attn: Code AT-7
Naval Weapons Evaluation Facility
Kirtland Air Force Base
Albuquerque, NM 87117

Commanding Officer
Attn: QEL
Naval Ammunition Depot
Concord, CA 94522

Superintendent Naval Academy
Attn: Library
Annapolis, MD 21402

Naval Plant Representative Office
Attn: SPL-332 (R. H. Guay)
Strategic Systems Project Office
Lockheed Missiles and Space Company
P. O. Box 504
Sunnyvale, CA 94088

Hercules Incorporated
Attn: Library
Allegany Ballistics Laboratory
P. O. Box 210
Cumberland, MD 21502

AMCRD
5001 Eisenhower Avenue
Alexandria, VA 22302

DISTRIBUTION (Cont.)

	Copies
Redstone Scientific Information Center Attn: Chief, Documents U. S. Army Missile Command Redstone Arsenal, AL 35809	2
Commanding Officer Attn: SARPA-TS-S #59 Picatinny Arsenal Dover, NJ 07801	
Commanding General Attn: BRL Aberdeen Proving Ground, MD 21005	
Commanding Officer Attn: Library Harry Diamond Laboratories 2800 Powder Mill Road Adelphi, MD 20783	
Armament Development & Test Center DLOSL/Technical Library Eglin Air Force Base Florida 32542	
Commanding Officer Naval Ordnance Station Louisville, KY 40124	
Director Attn: Library Applied Physics Laboratory Hopkins Road Laurel, MD 20810	
U. S. Department of Energy Attn: DMA Washington, DC 20545	
Director Defense Nuclear Agency Washington, DC 20305	

DISTRIBUTION (Cont.)

Copies

Research Director
Attn: R. W. Van Dolah
Pittsburgh Mining and Safety
Research Center
Bureau of Mines
4800 Forbes Avenue
Pittsburgh, PA 15213

Defense Documentation Center
Cameron Station
Alexandria, VA 22314 12

Goddard Space Flight Center, NASA
Glenn Dale Road
Greenbelt, MD 20771

Lawrence Livermore Laboratory
Attn: M. Finger
E. James
E. Lee
University of California
P. O. Box 808
Livermore, CA 94551

Sandia Laboratories
Attn: R. J. Lawrence, Div. 5166
P. O. Box 5800
Albuquerque, NM 87115

Director
Attn: Library
L. C. Smith
B. G. Craig
A. Popolato
Los Alamos Scientific Laboratory
P. O. Box 1663
Los Alamos, NM 87544

DDESB
Forrestal Building, Room GS 270
Washington, DC 20314

Aerojet Ordnance and Manufacturing
Company
9236 East Hall Road
Downey, CA 90241

DISTRIBUTION (Cont.)

Copies

Hercules Incorporated Research Center
Attn: Technical Information Division
B. E. Clouser
Wilmington, DE 19899

Thiokol/Huntsville Division
Attn: Technical Library
Huntsville, AL 35807

Shock Hydrodynamics Division
Attn: Dr. L. Zernow 2
Whittaker Corporation
4716 Vineland Avenue
North Hollywood, CA 91602

Stanford Research Institute
Attn: D. Curran
C. M. Tarver
333 Ravenswood Avenue
Menlo Park, CA 94025

Thiokol/Wasatch Division
Attn: Technical Library
P. O. Box 524
Brigham City, UT 84302

Thiokol/Elkton Division
Attn: Technical Library
P. O. Box 241
Elkton, MD 21921

Teledyne McCormick Selph
P. O. Box 6
Hollister, CA 95023

Lockheed Missiles and Space Division
1122 Jagels Road
Sunnyvale, CA 94086

R. Stresau Laboratory, Inc.
Star Route
Spooner, WI 54801

DISTRIBUTION (Cont.)

Copies

Rohm and Haas
Attn: H. M. Shuey
Huntsville, Defense Contract Office
723-A Arcadia Circle
Huntsville, AL 35801

U. S. Army Foreign Service
and Technology Center
220 7th Street, N. E.
Charlottesville, VA 22901

Princeton University
Attn: M. Summerfield
Department of Aerospace and
Mechanical Sciences
Princeton, NJ 08540

Pennsylvania State University
Attn: K. Kuo
Department of Mechanical Engineering
University Park, PA 16802

Ballistic Research Laboratories
Attn: N. Gerri
Aberdeen Proving Ground, MD 21005

Paul Gough Associates
1048 South Street
Portsmouth, NH 03801

Hercules Incorporated, Bacchus Works
Attn: M. Beckstead
P. O. Box 98
Magna, UT 84044

Professor H. Krier
A & A Engineering Department
101 Transporation Building
University of Illinois
Urbana, IL 61801

Chemical Propulsion Information Agency
The Johns Hopkins University
Applied Physics Laboratory
Johns Hopkins Road
Laurel, MD 20810

DISTRIBUTION (Cont.)

Copies

IIT Research Institute
Attn: H. S. Napadensky
10 W 35th Street
Chicago, IL 60616

Erion Associates, Inc.
Attn: W. Petray
600 New Hampshire Avenue,
Suite 870
Washington, DC 20037

NDW-NSWC(W)-5605/1 (Rev. 1-75)

TO AID IN UPDATING THE DISTRIBUTION LIST FOR NAVAL SURFACE WEAPONS CENTER, WHITE OAK LABORATORY TECHNICAL REPORTS PLEASE COMPLETE THE FORM BELOW:

TO ALL HOLDERS OF NSWC/WOL TR 77-175
by Donna Price, Code CR-10
DO NOT RETURN THIS FORM IF ALL INFORMATION IS CURRENT

A. FACILITY NAME AND ADDRESS *(OLD) (Show Zip Code)*

NEW ADDRESS *(Show Zip Code)*

B. ATTENTION LINE ADDRESSES:

C.

☐ REMOVE THIS FACILITY FROM THE DISTRIBUTION LIST FOR TECHNICAL REPORTS ON THIS SUBJECT.

D.
NUMBER OF COPIES DESIRED _____

GPO 885-970